Invited Review, to appear in 1999 December PASP

Search Techniques for Distant Galaxies

Daniel Stern & Hyron Spinrad
Department of Astronomy, University of California at Berkeley
Berkeley, CA 94720
email: (dan,spinrad)@bigz.berkeley.edu

ABSTRACT

How and when do galaxies form? Studies of the microwave background radiation reveal that the Universe is spectacularly homogenous at redshift $z \approx 1000$. Observations of the local Universe reveal that by $z = 0$ much of the luminous matter has condensed into mature, gravitationally-bound structures. One of the primary challenges to astronomers today is to achieve a robust understanding of this process of galaxy formation and evolution. Locating and studying young galaxies at large look-back times is an essential aspect of this program.

We review the systematic observational techniques used to identify galaxies at early cosmic epochs. In the past few years, the study of normal, star-forming galaxies at $z > 3$ has become possible; indeed, successful methods have been developed to push the frontier past $z = 5$. We are now directly observing individual galaxies within a Gyr of the Big Bang. We present a detailed review of the many search methods used for identifying distant galaxies, consider the biases inherent in different search strategies, and discuss early results of these studies. We conclude with goals for future studies at the start of the $21st$ century.

1. Introduction

At redshift $z \approx 1000$, the distribution of matter in the Universe was remarkably smooth: density fluctuations in the cosmic microwave background were of order one part in 10^5 on the degree scale (e.g., Bennett et al. 1996). Locally, 13 h_{50}^{-1} Gyr later at $z = 0$, we observe that the distribution of baryonic matter on the Mpc-scale is far from smooth, with baryons largely consigned to luminous, bound structures, such as galaxies and clusters of galaxies. These present-day structures can be explained by the gravitational collapse and coalescence of the overdense regions of the early Universe. A detailed understanding of this collapse, identified as galaxy and large-scale structure formation, is uncertain currently, and stands as one of the primary challenges to astrophysicists today.

The earliest epoch of galaxy formation lies beyond a redshift of 5. Recent observations have, for the first time, directly measured systems at the large lookback times implied by $z > 5$ (e.g., Dey

et al. 1998; Weymann et al. 1998; Spinrad et al. 1998; Chen, Lanzetta, & Pascarelle 1999; van Breugel et al. 1999; Hu, McMahon, & Cowie 1999). Several lines of evidence support a substantial epoch of galaxy formation prior to $z = 5$: the presence of metals (in excess of the primordial abundances) in high-z damped Lyα systems (e.g., Lu et al. 1996), quasars (Hamann & Ferland 1999), and star-forming galaxies at $z \sim 2.5 - 3.5$ (Steidel et al. 1996a; Lowenthal et al. 1997) requires metal creation and dispersal at higher redshifts. The tight photometric sequences in both low-z and intermediate-z clusters also attests to high formation redshift z_f at least for the elliptical galaxy formation in dense environments (e.g., Stanford, Eisenhardt, & Dickinson 1995). Indeed, some ellipticals at $z \sim 1.5$ are observed to contain evolved stellar populations with ages in excess of 3.5 Gyr (e.g., Dunlop et al. 1996; Spinrad et al. 1997; Dey et al. 2000), again implying high formation redshifts.

Theoretical paradigms of galaxy formation are vastly different: do large galactic spheroids form primarily via the monolithic collapse of a protogalactic cloud (e.g., Eggen, Lynden-Bell, & Sandage 1962) or are they built up through the hierarchical accretion of a multitude of subgalactic clumps (e.g., Baron & White 1987; Baugh et al. 1998)? Both faint number counts and the apparent lack of massive red systems at $z \gtrsim 1$ in (K-selected) redshift surveys would seem to favor the latter model (Kauffmann & Charlot 1998). However, the most direct answer will come with detailed studies of protogalaxies in the early Universe.

Considerable astronomical expertise and resources have been levied at identifying protogalaxies in the early Universe over the past 40 years (for a recent review, see Pritchet 1994). Table 1 lists the most distant galaxy confirmed as a function of time (see Fig. 1). There are several established and innovative methods to locate the minority population of distant systems from the confusion of faint, intermediate-luminosity systems that dominate faint galaxy counts (at optical/near-infrared wavelengths). This manuscript presents a review of these techniques with some attention applied to the implications of the current studies and expectations for this line of research in the near future.

Progress in this field has accelerated with the advent of new facilities, notably the Keck telescopes. In §2 we present a brief historical review of distant galaxy studies followed by a discussion of protogalaxy searches at non-optical wavelengths in §3. In §4 we discuss several optical/near-infrared selection techniques for the 'normal' population of distant galaxies. The cosmological redshifting of the light from these distant systems implies that our ground-based optical/near-infrared window samples the rest-frame ultraviolet spectrum; in §5 we therefore discuss the results of recent space-based observations of the ultraviolet properties of the youngest galaxies locally, as detailed studies of these relatively bright systems can yield considerable insight into observations of the most distant systems. In §6 we discuss the biases in the protogalaxy search techniques. In §7 we detail some of the highlights of these studies. Finally, §8 summarizes the discussion and suggests the primary questions which may occupy workers in this field at the start of the new millennium.

Throughout this paper, unless otherwise explicitly stated, we adopt an Einstein-de Sitter cosmology with a Hubble constant $H_0 = 50\ h_{50}$ $\mathrm{km\,s^{-1}\,Mpc^{-1}}$and no cosmological constant, $\Lambda = 0$.

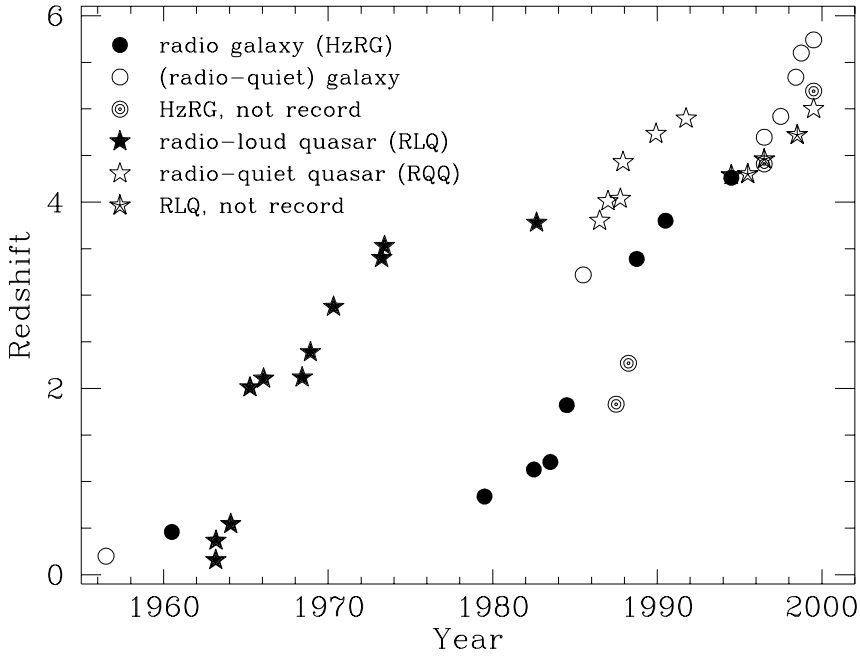

Fig. 1.— The highest-redshift object as a function of time. Note that the most distant quasars and galaxies were primarily selected from radio emission until recent years (1985 for quasars, 1997 for galaxies).

For this cosmology, the age of the Universe at redshift z is $\frac{2}{3}\ H_0^{-1}\ (1+z)^{-3/2} = 13.2\ h_{50}^{-1}\ (1+z)^{-3/2}$ Gyr. Magnitudes are quoted in the Vega-based system unless otherwise explicitly stated.

2. Historical Background: Brightest Cluster Galaxies

Historically, identifying galaxy clusters from overdensities on deep photographic plates was a proven method to find distant galaxies. Because the central cD galaxy in a cluster is quite luminous relative to the average galaxy (M_V(cD) ≈ -24 as opposed to $M_V^* \approx -21.5$ for early-type galaxies in clusters), clusters are excellent high-luminosity landmarks for studying the extragalactic Universe and were used by astronomers from 1950 to 1980 to find galaxies out to $z \approx 0.6$. While no longer primary sites for identifying distant galaxies directly because clusters require a substantial fraction of the Hubble time to form and virialize, they are once again becoming important for studying the process of structure formation. Eke, Cole, & Frenk (1996) show that the evolution of cluster abundances is sensitive to basic cosmological parameters. The temporal evolution of the co-moving galaxy cluster number density is determined by the rate of growth of large density perturbations. This depends mostly on the value of Ω; in a low-density universe the cluster population evolves slowly at low to intermediate redshift. In a critical ($\Omega = 1$) universe the density fluctuations continue to grow to the present epoch — thus, the cluster population is still evolving and we

Table 1: The Highest-Redshift Galaxy

Month/Year	Galaxy	z	Search Technique	Reference
1999	SSA22−HCM1	5.74	narrow-band imaging	Hu et al. (1999)
1998 Oct	HDF 4-473.0	5.60	photometric selection	Weymann et al. (1998)
1998 May	0140+326 RD1	5.34	serendipity	Dey et al. (1998)
1997	Cl 1358+62, G1/G2 arcs	4.92	serendipity/grav. lensing	Franx et al. (1997)
1996	BR 1202−0725 companion	4.70	narrow-band imaging	Petitjean et al. (1996)
1994	8C 1435+63	4.26	radio selection	Lacy et al. (1994)
1990	4C 41.17	3.80	radio selection	Chambers, Miley, & van Breugel (1990)
1988	B2 0902+34	3.39	radio selection	Lilly (1988)
1985	PKS 1614+051 companion	3.215	narrow-band imaging	Djorgovski et al. (1985)
1984	3C 256	1.82	radio selection	Spinrad & Djorgovski (1984)
1983	3C 324	1.206	radio selection	Spinrad & Djorgovski (1983)
1982	3C 368	1.131	radio selection	Spinrad (1982)
1979	3C 6.1	0.840	radio selection	Smith et al. (1979)
1976	3C 318	0.752	radio selection	Spinrad & Smith (1976)
1975	3C 411	0.469	radio selection	Spinrad et al. (1975)
1960	3C 295	0.461	radio selection	Minkowski (1960)
1956	Cl 0855+0321	0.20	cluster selection	Humason, Mayall, & Sandage (1956)

Notes.— Status as of 1999 August. Tabulation restricted to confirmed spectroscopic sources. In particular, Hu, Cowie, & McMahon (1998) recently reported a likely (serendipitously-discovered) candidate at $z = 5.63$ while Chen et al. (1999) report a candidate at $z = 6.68$ selected from deep *HST*/STIS grism spectroscopy. The authors deem both redshift determinations tentative with the current data (see Stern et al. 1999b). Note that Petitjean et al. (1996) refers to the spectroscopic confirmation of the $z = 4.7$ quasar companion initially identified by Djorgovski (1995) and Hu, McMahon, & Egami (1996). Many sources with potentially higher photometric redshifts have been identified, but await spectroscopic confirmation.

should expect more clusters locally than at intermediate redshift ($z \simeq 0.8$). Preliminary results from deep X-ray surveys do not indicate significant evolution in the galaxy cluster population from $z \simeq 0.8$ to the local Universe, suggestive of a low-Ω Universe (e.g., Rosati 1999).

The gravitational lensing caused by massive galaxy clusters amplifies the apparent brightness of background sources. Several galaxies at $z > 4$ have now been identified behind Abell clusters (e.g., Frye & Broadhurst 1998), with the most distant strongly-lensed source a serendipitously-discovered system at $z = 4.92$ (Franx et al. 1997).

3. Searches at Non-Optical Wavelengths

While optical and infrared techniques are usually needed to adequately image distant galaxies and measure their redshifts, the candidates may initially be located by observations in less-classical wavebands. We discuss identifying galaxies at non-optical wavelengths in the following subsections,

beginning with radio selection which has the richest history, and gradually moving to higher-energy photons.

3.1. High-Redshift Radio Galaxies

Powerful radio galaxies have proven to be good targets as luminous, presumably massive galaxies at large distance. They are spatially rare and usually luminous over many decades of the electromagnetic spectrum. As is clear from Table 1, until only recently, studies of the highest-redshift galaxies were synonymous with studies of high-redshift radio galaxies (HzRGs).

After the pioneering radio-optical identifications by Baade, Minkowski, Wyndham, Sandage, Ryle, Kristian, Longair, and Gunn, it became clear that relatively nearby powerful radio galaxies ($P_{408\mathrm{MHz}} > 10^{28}$ W Hz^{-1}) were usually associated with giant elliptical (gE and cD) galaxies (Matthews, Morgan, & Schmidt 1964). Upon closer inspection, a more precise description is that powerful radio sources are identified with disturbed-looking ellipticals of high luminosity (see Fig. 2) and that optical absolute magnitude (M_V) correlates with radio power ($P_{1.4\mathrm{GHz}}$) such that the brightest early-type (giant elliptical) galaxies are much more likely to host a radio source of significant power. Could this trend be exploited to find massive galaxies at high redshift?

The first major effort concentrated on the hosts of radio sources from the revised *3rd* Cambridge catalog (3CR; Bennett 1961), representing the brightest radio sources in the Northern hemisphere ($S_{178\mathrm{MHz}} > 9$Jy; $\delta > -5°$). Follow-up identifications by Longair, Gunn, Kristian, Sandage, Spinrad, and collaborators (c.f., Djorgovski et al. 1988) has lead to nearly complete spectroscopic redshift identification for the 328 radio galaxies in the 3CR catalogue. Only one faint galaxy, the host of 3C 249, remains without a definite spectroscopic redshift. The highest redshift belongs to 3C 257, a faint system ($K = 18.4$) at $z = 2.474$ (van Breugel et al. 1998). Lilly & Longair (1982, 1984) found a good correlation between the 2.2μm (K-band) infrared magnitude and galaxy redshift for powerful radio galaxies from the 3CR. At the redshifts of the 3CR, the K-band samples long-wavelength light, thought to be less-heavily affected by young stars and AGN; it was initially hoped that the K-band flux correlated tightly with mass and that the HzRGs were tracking the evolution of early-type galaxies. This discovery of a tight infrared Hubble, or $K - z$, diagram briefly suggested that radio galaxies might be good standard candles even if located at large redshift and thus become a viable tool for measuring basic cosmological parameters, such as q_0. Though this line of research later proved unfruitful, HzRGs still generally obey the $K - z$ relation out to the highest accessible redshifts currently probed (see Fig. 3), despite significant morphological evolution (van Breugel et al. 1998) and the dramatic k-correction effects (K samples rest-frame U at $z \sim 5$).

To identify higher-redshift HzRGs and remove the redshift–radio power degeneracy in studies of HzRGs, several contemporary efforts have concentrated on lower flux density limit samples. Recent mJy surveys include the Molonglo Reference Catalog (MRC; McCarthy, Baum, & Spinrad 1996), the MIT-Green Bank survey (Stern et al. 1999b), and Cambridge surveys (e.g., 6C; Hales, Baldwin,

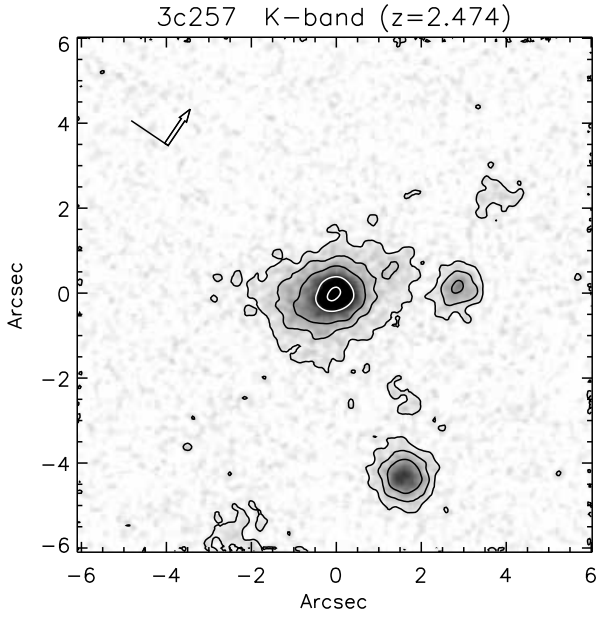

Fig. 2.— Near-infrared image of the HzRG 3C 257 at $z = 2.474$, obtained with the NIRC camera on Keck I. 3C 257 is the highest-redshift radio galaxy identified from the 3CR survey. Panel is $12\farcs0$ square, centered on the HzRG and oriented such that the inner radio axis is parallel to the abscissa. The compass arrow in the upper left indicates NE orientation, with north shown by the heavier arrow. The lowest contour corresponds to a surface brightness of 21.6 mag arcsec^{-2}. Note that the morphology is well-described by a deVaucoleurs $r^{1/4}$ profile, as expected for an early-type system. Figure courtesy van Breugel et al. (1998).

& Warner 1993). Additional efforts have concentrated on μJy samples such as the Leiden Berkeley Deep Survey (Neuschaefer & Windhorst 1995) and sensitive radio maps of the Hubble Deep Field (Richards et al. 1998). These studies have shown that radio luminosity weakly correlates with emission line luminosity (Rawlings et al. 1989; Baum & Heckman 1989), that weak radio galaxies do not generally contain significant non-thermal light in their optical spectra (Keel & Windhorst 1991), that the alignment effect (discussed below) becomes less pronounced with lower radio flux density samples (e.g., Rawlings & Saunders 1991; Dunlop & Peacock 1993; Eales & Rawlings 1993), and that radio power apparently correlates with ionization state in HzRGs (Stern et al. 1999b).

To identify the highest-redshift HzRGs, two techniques have recently been exploited with considerable success, yielding the first detection of an HzRG at $z > 5$: TN J0924−2201 at $z = 5.19$ (van Breugel et al. 1999). First, empirically, HzRGs with ultra-steep spectra (USS; for $S_\nu \propto \nu^\alpha$, $\alpha \lesssim -1.3$) at radio wavelengths tend to be at higher redshifts (e.g., Chambers et al. 1990). All HzRGs at $z > 3.8$ have been identified by targeting USS samples. A partial explanation for this technique derives from the observation that the most powerful radio galaxies locally have

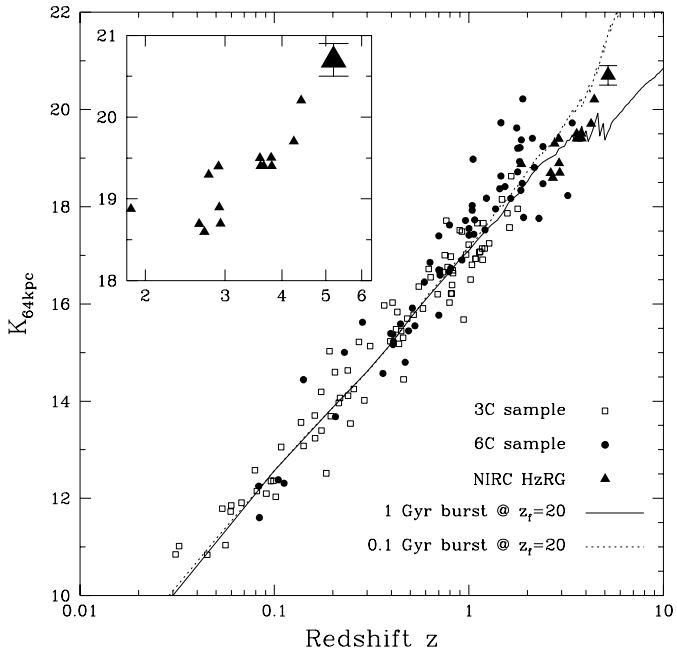

Fig. 3.— Hubble $K-z$ diagram for HzRGs. Small filled triangles are Keck/NIRC measurements of HzRGs from van Breugel et al. (1998), the large filled triangle with error bars represents TN J0924−2201 at $z = 5.19$ (van Breugel 1999), currently the most distant HzRG known, and all other photometry is from Eales et al. (1997). Magnitudes are aperture-corrected to a 64 kpc metric diameter using $H_0 = 65\,\mathrm{km\,s^{-1}\,Mpc^{-1}}$ and $\Omega_0 = 0.3$. The inset highlights this empirical relation at the highest accessible redshifts currently. Two stellar evolutionary models from Bruzual & Charlot (1993) with formation redshifts $z_f = 20$ and normalized at $z < 0.1$ are plotted. Figure courtesy van Breugel et al. (1999).

radio spectral energy distributions which steepen with frequency (e.g., Carilli & Yun 1999). The k-corrections therefore imply that sources at increasing redshifts exhibit steeper radio spectral indices at a given observed frequency. The second technique relies on selecting those USS radio sources whose hosts have the faintest observed K magnitudes and thus, according to the $K-z$ diagram (Fig. 3), are likely associated with the most distant systems. De Breuck et al. (1999) have recently constructed a full-sky USS sample ($\alpha^{1.4\mathrm{GHz}}_{365\mathrm{MHz}} < -1.3$). TN J0924−2201 at $z = 5.19$, a $1\farcs2$ radio double with $S_{4.85\mathrm{GHz}} = 8.6 \pm 0.5$ mJy, $\alpha^{1.4\mathrm{GHz}}_{365\mathrm{MHz}} = -1.63 \pm 0.08$, and $K = 21.3 \pm 0.3$ ($2\farcs1$ diameter circular aperture), is among the steepest-spectrum USS sources from the De Breuck et al. (1999) sample and has among the faintest K-band magnitudes of the subsample with infrared imaging (van Breugel et al. 1999). Table 2 lists several physical parameters for all HzRGs at $z > 3.8$ in the literature currently. At the time of this writing, the authors are aware of 22 HzRGs at $z > 3$, including five at $z > 4$ and one at $z > 5$. We note, however, that K-band imaging is not the Rosetta Stone of HzRG studies; spectroscopy of several HzRGs with faint K-band identifications (e.g., $K \gtrsim 20$) reveal lower redshift systems, thus defying a simple one-to-one translation of K-band magnitude to redshift (e.g., Eales & Rawlings 1996).

Table 2: Physical Parameters of High-Redshift Radio Galaxies at $z > 3.8$

Galaxy	z	$\alpha_{365\mathrm{MHz}}^{1.4\mathrm{GHz}}$	K (mag.)	$S_{1.4\mathrm{GHz}}$ (mJy)	$L_{\mathrm{Ly}\alpha}$	$W_{\mathrm{Ly}\alpha}^{\mathrm{rest}}$ (Å)	Reference
TN J0924−2201	5.19	−1.63	21.3	73	0.8	$\gtrsim 115$	van Breugel et al. (1999)
VLA J123642+621331	4.42	−0.94	21.4	0.432	0.1	$\gtrsim 50$	Waddington et al. (1999)
6C 0140+326	4.41	−1.15	20.7	92	7.7	700	Rawlings et al. (1996)
8C 1435+63	4.25	−1.31	20.1	498	2.3	670	Spinrad, Dey, & Graham (1995)
TN J1338−1942	4.11	−1.31	20.3	123	14.4	200	De Breuck et al. (1999)
4C 41.17	3.80	−1.25	20.7	266	9.0	100	Dey et al. (1997)

Notes.— Lyα luminosity, $L_{\mathrm{Ly}\alpha}$, is in units of $10^{43} h_{50}^{-2}\,\mathrm{ergs\,s^{-1}}$. $W_{\mathrm{Ly}\alpha}^{\mathrm{rest}}$ is the rest-frame Lyα equivalent width. The discovery papaers for 8C 1435+63 and 4C 41.17 were Lacy et al. (1994) and Chambers et al. (1990) respectively.

The radio morphologies of HzRGs often have a double-lobed structure. At low-redshift, optical images of radio galaxies often show signs of recent mergers, as evidenced by multiple nuclei and subtle shells around some symmetric early-type galaxies to dramatic tidal tails around others (e.g., Rigler et al. 1992). At $z \gtrsim 0.7$, the optical axis of the host galaxy is typically aligned with the radio axis (Chambers, Miley, & van Breugel 1987; McCarthy et al. 1987). Optical and radio major axes usually differ by less than 20°. This alignment is most noticeable in emission-line images: nearly all of the emission line regions of HzRGs in the 3CR sample are well-aligned with their radio axis (McCarthy, Spinrad, & van Breugel 1995). At $z > 0.7$ the rest-frame ultraviolet continua are also strongly aligned. At observed near-infrared wavelengths, the alignment is less pronounced. Lower-redshift radio galaxies often have regular $r^{1/4}$ profiles in the K-band (e.g., Best, Longair, & Röttgering 1996), while at the high-redshift end, van Breugel et al. (1998) find peculiar K-band morphologies — faint, large-scale (~ 50 kpc) emission often surrounding multiple-compact components aligned with the radio axis.

One interpretation of the alignment effect is that it is dominated by a blue-component, which has variously been attributed to emission from young, hot stars, scattered light from an active galactic nucleus (AGN; a buried quasar or a buried mini-quasar), or nebular continuum emission from clouds excited by an obscured nucleus (Dickson et al. 1995). Spectropolarimetric studies have convincingly demonstrated that extended, aligned ultraviolet (UV) emission in HzRGs at $z \sim 1-2$ is often strongly polarized, with the electric vector perpendicular to the major axis of the UV emission (e.g., Jannuzi et al. 1995; Dey et al. 1996; Cimatti et al. 1996, 1997). These observations strongly indicate that much of the observed UV light is AGN light which has been scattered into our line of sight by dust and/or electrons in the ambient medium. Other galaxies, notably 4C 41.17 at $z = 3.80$ (Dey et al. 1997), exhibit no polarized continuum in the aligned emission, but do show stellar absorption features (e.g., S Vλ 1502), indicating that (jet-)induced star formation is important in some HzRGs. The true scenario is likely a combination of these processes.

The observed infrared, sampling the rest-frame visible or UV for large redshifts, is thought to

be dominated by starlight from the host galaxy; deductions made from the H- or K-bands might then be compared to other large galaxies of stars. The robustness of this conclusion is still unproven (e.g., see McCarthy 1999). To settle the point we need to observe stellar spectral features in the near-infrared, but spectroscopy of faint ($K \gtrsim 19$) galaxies at 2μm is technically difficult, even with the largest telescopes. However, the uniformity of the $K - z$ diagram (Fig. 3) suspiciously traces the rapid formation of a massive galaxy of stars at high redshift, similar to expectations for the formation and evolution of early-type galaxies.

We now ask a more difficult question: can the study of distant radio galaxies tell us about the youthful galaxy population in general? Until recently, HzRGs were the only stellar systems known at $z > 3$. However, modern photometric studies of deep imaging fields (discussed in detail in §4) have led to the discovery of a population of normal, star-forming galaxies at comparably large distances. At $z \sim 3$ the HzRGs are rather larger and more luminous than these field galaxies: a typical powerful radio galaxy at $z \sim 3$ has $K \approx 19$, while the normal, star-forming, field galaxies at $z \sim 3$ typically have $K \approx 22$, some 3 magnitudes fainter. At $z \sim 3$ the HzRGs are typically spatially extended by $1 - 2$ arcseconds at K, while the young, field galaxies are generally barely resolved in space-based (optical) images (half-light radii of $0\farcs2 - 0\farcs3$; Giavalisco, Steidel, & Macchetto 1996). Assuming the observed K-band light is dominated by stars in both cases, it would take ~ 15 young field galaxies to match the luminosity of a powerful radio galaxy at $z \sim 3$. Could it be that the HzRGs were the first objects to form in the early Universe? If so, what is the significance of the massive black hole that is thought to reside at the HzRG nucleus and power the synchrotron emission at radio wavelengths? Is it primordial, or the result of galaxy evolution in the early Universe? Extending the frontiers of distant galaxy studies of both the young, star-forming systems and the HzRGs to earlier cosmic epochs will be a valuable enterprise. Eventually, as we probe to the epoch in which the (proto-)elliptical hosts of HzRGs are being constructed by galaxy mergers, we might expect to see diminishing systematic differences in the long-wavelength luminosities of HzRGs and star-forming galaxies.

Optical spectroscopy of a few (lower-power) HzRGs at $z \approx 1.5$ have shown spectra devoid of the narrow, high-equivalent width emission lines which typically dominate HzRG spectra. Detailed studies of two galaxies (LBDS 53W091 and LBDS 53W069 — Dunlop et al. 1996; Spinrad et al. 1997; Dey et al. 2000) show that their observed optical spectra are well-represented by an evolved stellar population of age $\gtrsim 3.5$ Gyr (see Fig. 4), with distinctive continuum decrements evident at 2640 Å and 2900 Å whose amplitudes are similar to those seen in late F-type stars. Though the modeling of the rest-frame UV spectra are uncertain currently — different spectroevolutionary models of a solar metallicity system with a delta function star formation history yield significantly different inferred ages (see Spinrad et al. 1997) — the hypothesis that these systems have ages a substantial fraction of the Hubble time at their observed redshifts seems unassailable. These systems are among our best examples of giant elliptical galaxies at $z > 1$.

The modest surface density of faint-/moderate-strength radio sources reminds us of their rarity at any redshift: the surface density of radio sources with flux densities $S_{1.4\mathrm{GHz}} > 1$ mJy (i.e., a

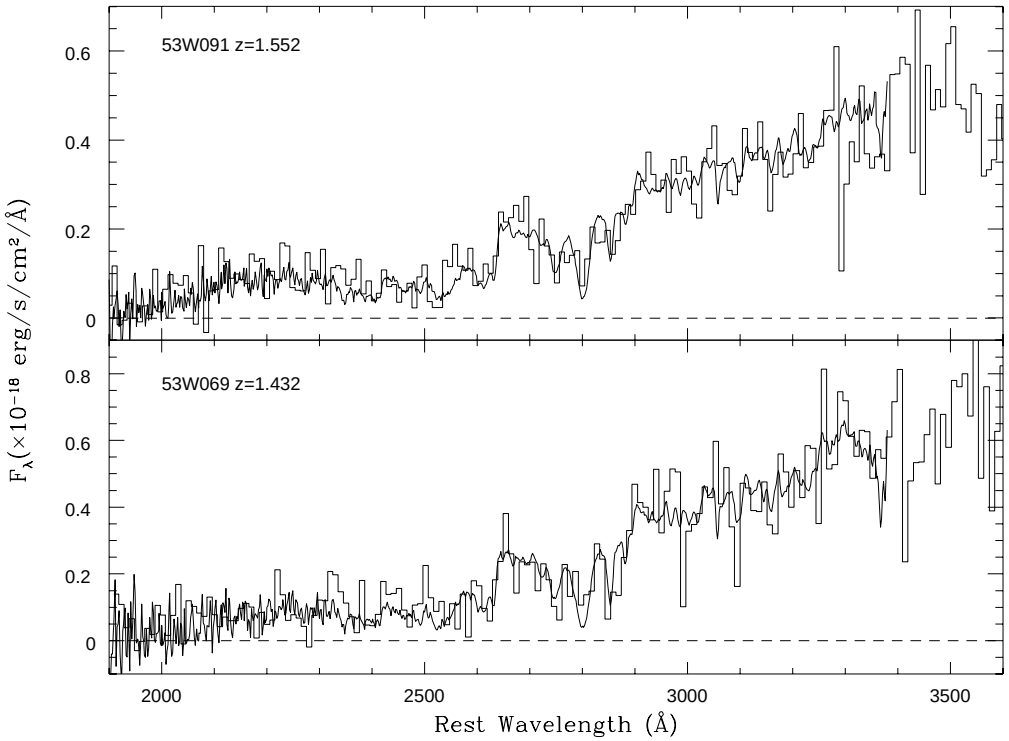

Fig. 4.— Keck spectra of the two oldest known high-redshift galaxies. The upper panel shows the spectrum of 53W091 (histogram) overlaid with the mean spectrum of an F6V star from the Wu et al. (1991) *IUE* Spectral Atlas. The bottom panel shows the spectrum of 53W069 (histogram) compared with the mean spectrum of an F9V star. Since the UV spectrum of coeval populations is dominated by light from main-sequence turnoff stars, these fits imply ages of 3.5 Gyr for 53W091 and 4.5 Gyr for 53W069. These ages agree with those derived from more-detailed population synthesis. Figure courtesy Dey (1999).

moderately weak radio flux) is $\lesssim 0.03$ sources per square arcminute (Becker, White, & Helfand 1995). The co-moving density of HzRGs is estimated to be $10^{-8}h_{50}^3$ galaxies Mpc^{-3} at $z \sim 3$ (e.g., Dunlop & Peacock 1990). For reference, the co-moving density of early-type galaxies locally is $\sim 2 \times 10^{-4}h_{50}^3$ Mpc^{-3} (Cheng & Krauss 1999).

Even if HzRGs prove not to be identified with an early stage in the formation of all early-type galaxies, they remain convenient beacons for large, overdense regions, populated by smaller normal galaxies and are likely to be important for studies of the formation and evolution of large scale structure. Several galaxy clusters at $z \approx 1$ have been identified around distant radio galaxies (e.g., Dickinson 1995; Deltorn et al. 1997), with associated high-density regions located even out to $z = 2.4$ (Pascarelle et al. 1996; Francis et al. 1996; Pentericci et al. 1997; Carilli et al. 1998).

For a review of HzRGs, see McCarthy (1993). We now consider high-redshift galaxies selected at other non-optical/infrared wavelengths. Selecting targets at other wavelengths has the potential to pick out the rare beast in the cosmos, which, from a Galilean world view, is apt to be far away.

3.2. Sub-mm Detections of Distant Galaxies

Sub-mm identifications and observations of distant galaxies has recently been energized by array detectors, most notably the Sub-Millimeter Common User Bolometer Array (SCUBA; Holland et al. 1999) on the 15-m James Clerk Maxwell Telescope on Mauna Kea. SCUBA has enabled the first deep, unbiased surveys to be made of the sub-mm sky (generally implemented at 850μm). Sub-mm observations are particularly sensitive to dust emission, associated with re-processed light from young, high-mass stars in galaxies undergoing massive bursts of star formation. The thermal dust spectrum peaks at a rest-frame wavelength of around 100μm which has the interesting result of *negative* sub-mm k-corrections: the redshifted, modified black body spectrum is sufficient to offset cosmological dimming for $\Omega_0 = 1$ and $1 \lesssim z \lesssim 10$! Even for low values of Ω_0, the 850μm flux density is only expected to decrease by a factor of a few over this redshift range (Blain & Longair 1993; Hughes et al. 1998). Dusty, starburst galaxies can therefore be selected at $z \gtrsim 1$ in an almost distance-independent manner. Several relatively bright sources have recently been identified (e.g., Smail, Ivison, & Blain 1997; Barger et al. 1998, 1999; Hughes et al. 1998) and the flux densities may occasionally imply immense star-formation rates in excess of 1000 $M_\odot$ yr^{-1} (e.g., Dey et al. 1998)! A new question is what fraction of young galaxies are dusty enough to re-emit strongly at $\lambda_{\rm rest} \approx 100\mu$m? In particular, do the sub-mm galaxies constitute an orthogonal population to the star-forming, UV-bright galaxies considered in §4?

The main difficulty in the current interpretation of weak extragalactic sub-mm sources is the relatively large (15″) beam size of SCUBA at 850μm. The issue is reminiscent of the early days of follow-up work on radio sources: sub-mm field sources have uncertain identifications. For example, the Hughes et al. (1998) deep 850μm observations of the Hubble Deep Field (HDF) detects five sources to a limiting flux density of 2 mJy, corresponding to a surface density of ~ 0.9 sub-mm sources per square arcminute to this limiting brightness. The sources are likely to be associated with individual (starburst) galaxies over a large redshift range, with some contribution of AGN likely. The critical point is, of course, which galaxies? And what are their redshifts? Hughes et al. (1998) suggest that one source (HDF850.4; $S_{850\mu{\rm m}} = 2.3 \pm 0.5$ mJy) is associated with an extreme starburst galaxy (HDF 2-339.0; $I_{814}^{\rm AB} = 23$) at $z \simeq 1$, whilst the other four sub-mm sources could be identified with more distant galaxies, perhaps out to $z \approx 4$. However, recent deep high-angular resolution radio observations of the HDF by Richards (1999) suggest alternate identifications of the sub-mm sources: translating the astrometric center of the sub-mm map by 6″ increases the number of radio identifications of sub-mm sources from one out of five to four out of five. If correct, this would then suggest that the presently detectable sub-mm sources in the HDF are restricted to $z \lesssim 2$.

Carilli & Yun (1999) show that the radio-to-sub-mm spectral index is a viable redshift indicator for star-forming galaxies. Using semianalytic models and the well-studied local starburst galaxies M82 and Arp 220, they show that the 1.4 GHz to 850 μm (350 GHz) spectral index $\alpha_{1.4\ {\rm GHz}}^{850\mu{\rm m}}$ increases with redshift; galaxies with $\alpha_{1.4\ {\rm GHz}}^{850\mu{\rm m}} \simeq 0.5$ are likely to be at $z \simeq 1$. Examining the Hughes et al. (1998) sub-mm identifications in the HDF, Carilli & Yun (1999) conclude that

most of the sources are at $z \simeq 1.5$. Carilli & Yun (1999) also show that the Richards (1999) $6''$ offset yields low-redshift identifications with inconsistently large radio-to-sub-mm spectral indeces, implying that the Hughes et al. (1998) astrometry is likely accurate.

Smail et al. (1997, 1998) report on sub-mm selected sources from a SCUBA cluster lens survey. Deep sub-mm imaging of clusters offers two advantages: first, gravitational lensing magnifies any background sources (a median amplification of ~ 2.5 is reported for this survey), making spectroscopic follow-up easier. Second, gravitational lensing increases the mean separation of background sources, thus diminishing source confusion. Barger et al. (1999) reports on a spectroscopic follow-up study of the possible optical counterparts and suggest that the majority of the sub-mm sources reside at $z < 3$. This implies that the far-infrared and sub-mm background light recently measured from the *FIRAS* and *DIRBE* experiments on the *COBE* satellite (e.g., Schlegel, Finkbeiner, & Davis 1998) are emitted by sources at $z < 3$. Furthermore, this work suggests that the peak activity in heavily obscured (dusty) sources (both AGN and starbursts) lies at relatively modest redshift.

In the absence of high-angular resolution sub-mm capabilities, this new field enjoys considerable uncertainties. Further research is clearly needed, and we can look forward to rapid progress in understanding the redshift distribution, host galaxy properties, dust properties, and evolution of the sub-mm population in the near future as the next generation of mid-IR/sub-mm instruments (e.g., SCUBA+, BOLOCAM) become available.

3.3. Luminous Infrared Galaxies

The first all-sky, far-infrared survey, conducted in 1983 by the *Infrared Astronomical Satellite* (*IRAS*), detected the existence of a large population of galaxies which emit more energy in the infrared ($\sim 5 - 500\mu$m) than at all other wavelengths combined. In the local Universe ($z \lesssim 0.3$), these luminous infrared galaxies (LIRGs) are the dominant population of sources with luminosities above $10^{11} L_{\odot}$, being more numerous than quasars, Seyferts, and optically-selected starbursts at comparable bolometric luminosity. Morphological studies show that LIRGs are triggered by gas-rich galaxy collisions and mergers. The bulk of the infrared flux is powered by dust heating from a massive starburst within giant molecular clouds. At the highest luminosities, energy input from active galactic nuclei becomes important, and LIRGs may represent an important stage in the formation of quasars and powerful radio galaxies. LIRGs may also be an important phase in the formation of elliptical galaxies, globular clusters, and in the metal enrichment of the intergalactic medium. For a recent review of LIRGs, see Sanders & Mirabel (1996).

In terms of studying distant galaxies, the *IRAS* sample of LIRGs has not provided many sources. The vast majority of *IRAS* LIRGs are at relatively modest redshift ($z \lesssim 0.4$). Only two *IRAS* sources have been identified at $z > 2$: *IRAS* Faint Source 10214+4724 at $z = 2.286$ (Rowan-Robinson et al. 1991) and the Cloverleaf quasar at $z \sim 2.5$. Both are gravitationally

lensed (e.g., Barvainis et al. 1994; Elston et al. 1994; Graham & Liu 1995; Eisenhardt et al. 1996), with inferred amplification-corrected luminosities similar to the local sample of LIRGs. Studying the unlensed population of these optically-obscured sources to higher redshift will be an important step towards understanding the formation and evolution of massive galaxies, but will require more sensitive infrared surveys and/or new search strategies. The *Space Infrared Telescope Facility* (*SIRTF*) is expected to identify LIRGs at cosmological distances. Some sub-mm sources are likely to be distant analogs of LIRGs.

3.4. X-ray Emission Associated with Distant Galaxies

Most normal galaxies are rather weak X-ray emitters, with spatially extended X-ray emission in the range of $\sim 10^{38}$ ergs s^{-1} to $\sim 10^{42}$ ergs s^{-1} (Fabbiano 1989). This emission largely derives from the hot phase of the interstellar medium (in early-type galaxies), close accreting binaries, and the end products of stellar evolution. Stellar coronal emission does not contribute significantly to the total X-ray output of normal galaxies. Extremely sensitive X-ray surveys, such as the 56 ksec *Röntgensatellit* (*ROSAT*) Deep Survey in the Marano field (Zamorani et al. 1999) and the 1.5 Msec *ROSAT* Deep Survey in the Lockman Hole (Hasinger et al. 1998; Schmidt et al. 1998), resolve most of the hard X-ray ($0.5 - 2$ keV) background into discrete sources. The majority of optically-identified X-ray sources are broad-lined AGN, i.e., quasars and Seyfert-II galaxies. Recent claims of a new population of X-ray emitting, narrow-emission line galaxies dominating faint X-ray counts (Georgantopoulos et al. 1996) are not supported by the deepest surveys (Hasinger et al. 1998).

Thus, X-ray surveys are not expected to be significant tools for identifying normal, distant galaxies, though they can identify distant AGN. The most-distant X-ray source known currently is the radio-loud quasar GB 1428+4217 at $z = 4.72$ identified due to its X-ray emission (Fabian et al. 1997).

X-rays are also emitted by bremsstrahlung radiation from the hot gas in intracluster media. Therefore, spatially-extended X-ray sources have considerable value in locating distant, over-dense regions of the Universe and are thus valuable probes for the formation and evolution of large scale structure. Eke et al. (1996) demonstrate that the evolution of the abundance of rich clusters is strongly dependent upon the cosmological density parameter Ω_0. Most X-ray clusters identified to date lie at $z \lesssim 0.5$. Stanford et al. (1997) and Rosati et al. (1999) report two spatially-proximate X-ray clusters at $z \approx 1.27$.

The *Chandra X-Ray Observatory* (formerly known as *AXAF*) and *X-Ray Multi-Mirror Mission* (*XMM*) will soon extend X-ray detections to lower flux limits, providing a valuable aid in the detection of very distant AGN and galaxy clusters.

3.5. Gamma-Ray Bursts

While the physical origin of gamma-ray bursts (GRBs) remains enigmatic, it is now clear that they have an extragalactic origin and are associated with an immense, possibly beamed, energy release. This makes them visible at large look-back times. Several GRBs have been credibly identified with X-ray, radio, and optical transients. Most spectacularly, GRB 990123 was identified with an optical transient whose peak apparent brightness 47 s after the γ-ray release was $9th$ magnitude in the optical, dimming by 5 mag within 500 s (Akerlof et al. 1999). As of this writing, nine GRBs have reliable spectroscopic redshifts, with one event (GRB 971214) identified with a galaxy at $z = 3.428$ (Kulkarni et al. 1998). Spectroscopy of the GRB 990123 optical transient reveals an absorption system with $z_{\rm abs} = 1.6004$ (Kelson et al. 1999), setting a minimum distance for that extremely bright source. Assuming unlensed isotropic energy release, the implied energies are immense (isotropic equivalent $E \gtrsim 10^{52\pm1}$ erg in the γ-rays alone). Thus, at least some fraction of GRBs are sufficiently powerful to be detected at great distances. The optical transients typically are not associated with the central nuclei of galaxies, implying that GRBs are not related to AGN or the massive black holes which are thought to reside in the centers of many galaxies (Bloom et al. 1999). The two leading theories suggest that GRBs are associated with the creation of a stellar-mass black hole, either through coalescence of the remnants of a massive stellar binary (e.g., neutron star–neutron star or neutron star–black hole; Paczynski 1986; Goodman 1986) or through direct collapse of a massive star (Woosley 1993; Paczynski 1998). Both models predict that GRBs should preferentially occur in star-forming galaxies. Follow-up observations of the faint host galaxies of GRBs may become a robust method of studying normal galaxies at the highest accessible redshifts. In particular, spectroscopy during the bright phase may yield redshifts which would be untenable or impossible for the faint hosts during their quiescent phase.

Fig. 5.— `See fig5.jpg.` Detail of the Keck/LRIS BRI and HST/NICMOS F160W ($\sim H$) images of the 0140+326 field. The images shown are $27\farcs5$ on a side, and north is up and east is to the left. Objects at high redshift can be systematically and robustly selected on the basis of redshifted Lyman line and continuum absorptions of hydrogen. The galaxies targeted as B-band 'dropouts' are labeled BD3 and BD12 and lie at $z = 4.02$ and $z = 3.89$ respectively. The serendipitously discovered $z = 5.34$ galaxy is labeled RD1 (R-band dropout; Dey et al. 1998) in this figure. 6C 0140+326 (Rawlings et al. 1996) was the most distant radio galaxy known at the time of the deep imaging and lies at $z = 4.41$. It is also a B-band dropout. Hydrogen absorption from the redshifted Lyman break and Lyα forest causes high-redshift objects to effectively disappear in the bluer passbands.

3.6. Summary

High-redshift sources identified at non-optical/near-infrared wavelengths therefore provide an important, albeit skewed, view of galaxy formation, typically selecting unusual sources with powerful active nuclei or systems undergoing massive bursts of star formation. Recently several optical/near-infrared techniques have proved successful at isolating the 'normal' population of distant galaxies. We discuss these methods below. In §6 we discuss the biases inherent in the various selection techniques, detailing how populations identified at differing wavelengths compare.

4. Optical/Near-Infrared Selection of Distant Galaxies

4.1. Lyman-Break Galaxies

In recent years our understanding of the earliest stages of galaxy formation and evolution has been revolutionized. With the commissioning of the Keck telescopes atop Mauna Kea and the availability of deep ground- and space-based imaging, the photometric technique outlined in Steidel & Hamilton (1992) has been used to routinely select high-redshift, star-forming systems. Dubbed the "Lyman-break" method, objects are identified on the basis of the redshifted continuum spectral discontinuity at $(1+z)\times912$ Å and relatively flat (in f_ν) continua long-ward of the redshifted Lyα (at $(1+z)\times1216$ Å), as we expect from hot O and B stars. At the largest redshifts ($z \gtrsim 4$), absorption due to the Lyα and Lyβ forests plays a role of equal or greater importance in attenuating the deep UV continua. These hydrogen absorptions from the Lyman limit and the Lyman forests cause high-redshift objects to effectively disappear in the bluer passbands. The technique is therefore sometimes referred to as the 'dropout' technique (see Fig. 5). U-band dropouts were initially used to chart the Universe at $z \sim 3$ (Steidel et al. 1996a, 1996b). This technique has now been pushed to higher redshifts: first to $z \gtrsim 4$ (Dickinson 1998; Dey et al. 1998; Steidel et al. 1999), and now finally above $z = 5$ ( );][]Weymann:98, Spinrad:98.

The hydrogen absorptions are ubiquitous: they are present in the spectra of O and B stars which will dominate the rest-frame UV continua of young, star-forming galaxies with conventional mass functions. They are also present for any system with a substantial hydrogen column present along our line of sight. In particular, bound-free absorption of hydrogen at the Lyman limit (at $(1+z)\times912$ Å) will severely truncate a background spectrum if the total neutral hydrogen column at the relevant wavelength exceeds $n_H \approx 3\times10^{17}$ cm^{-2}. Thus, Lyman absorption is expected even in systems whose spectral energy distributions are not dominated by hot, young stars; similar techniques have routinely been used to identify high-redshift quasars from deep multi-band imaging such as the Palomar Observatory Sky Surveys (e.g., Kennefick, Djorgovski, & de Calvalho 1995; Stern et al. 1999c) and the Sloan Digital Sky Survey (Fan et al. 1999).

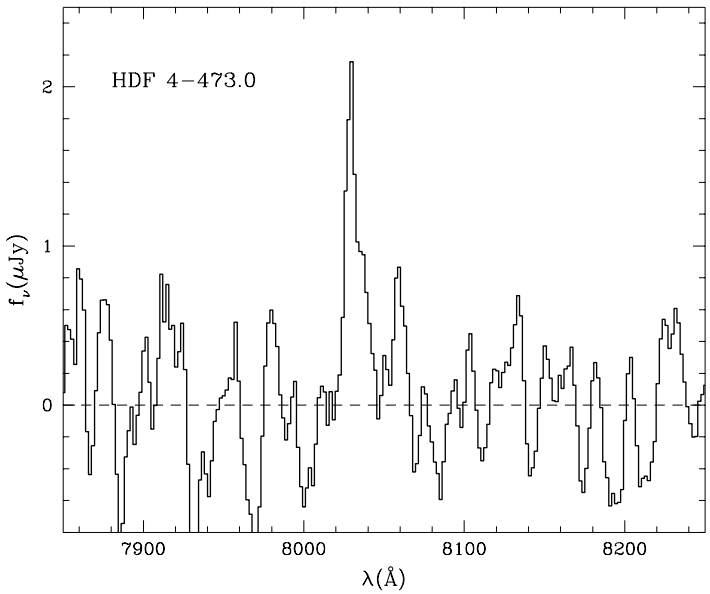

Fig. 6.— Spectrum of HDF 4-473.0. The total exposure time is 4 h. It was selected from the deep *HST* optical and near-infrared images of the HDF (Williams et al. 1996; Thompson et al. 1998) as a V_{606}-dropout ($V_{606} > 30$; $I_{814} = 27.1$ AB). The spectrogram shows a single emission line at 8029 Å. The asymmetric line profile and broad band colors are most consistent with this being Lyα at $z = 5.60$. Figure courtesy Weymann et al. (1998).

4.2. Photometric Redshifts

Lyman-break and Lyman-forest methods are just two examples of photometric redshift determinations, in which galaxy redshifts are estimated using multiband photometric information. The idea has a long history, dating back to Baum (1962) who used nine-band photoelectric data to estimate galaxy cluster redshifts. Koo (1985), analyzing four-band photographic data, showed that iso-redshift contours on color-color plots provide reliable photometric redshift estimates. Recently, photometric techniques have enjoyed a revival, largely catalyzed by the deep photometry of the HDF and the new generation of large-format CCD arrays. The typical redshift uncertainty for the photometric methods is expected to be in the range of $\Delta z = 0.05 - 0.10$. This accuracy is sufficient for many scientific goals, such as luminosity function determinations, luminosity density determinations, and projected correlation function analyses. The technique is also efficient for identifying unusual sources, such as distant galaxies, quasars, and galaxy clusters, which can then be targeted for detailed spectroscopic study.

Several teams are actively pursuing photometric redshift determinations and the HDF (recently augmented by the HDF-South) has been an excellent laboratory for validating the technique (c.f., Hogg et al. 1998). Table 3 lists some of the primary working groups with brief commentary on their technique. Fig. 7, comparing spectroscopic redshifts in the HDF with photometric red-

shift determinations by the Stony Brook group, illustrates the robustness of photometric redshift determinations. A recent review of photometric redshifts is presented in Yee (1998).

Table 3: Selected Groups Involved in Photometric Redshift Determinations

Group	Technique	Ref.
Berkeley	Bayesian analysis with empirical spectral templates	1
Imperial College	synthetic spectral templates	2
Johns Hopkins	empirical fit to 4-dimensional flux space	3
Princeton	empirical fit to 3-dimensional color space	4
Stony Brook	hybrid spectral templates	5
Toronto	hybrid spectral templates	6
Victoria	synthetic and empirical spectral templates	7

Notes.— References: (1) Benítez (1999); (2) Mobasher et al. (1996); (3) Connolly et al. (1995, 1997); Brunner et al. (1997); (4) Wang, Bahcall, & Turner (1998); (5) Lanzetta, Yahil, & Fernàndez-Soto (1996); Fernàndez-Soto, Lanzetta, & Yahil (1999); (6) Sawicki, Lin, & Yee (1997); (7) Gwyn & Hartwick (1996).

Contemporary photometric redshift determinations can be divided into two major strategies. The first approach (e.g., Koo 1985; Lanzetta et al. 1996; Gwyn & Hartwick 1996; Mobasher et al. 1996; Sawicki et al. 1997; Benítez 1999; Fernàndez-Soto et al. 1999) involves fitting observed galaxy colors with redshifted spectral templates. These templates may be empirical, synthetic, or hybrid, and may be modified by dust absorption and/or the redshift-dependent opacity of intergalactic hydrogen. Statistical treatments are used to determine a redshift distribution function, generally quoted as a single number corresponding to the peak of the distribution. However, determinations of, for example, galaxy luminosity functions, should retain the photometric redshift distribution function to reliably indicate the uncertainties of the analysis. The other approach (e.g., Connolly et al. 1995; Brunner et al. 1997; Connolly et al. 1997; Wang et al. 1998) is purely empirical: with a sufficiently large training set, an empirical relation between redshift and observed magnitudes m_0 and colors C can be determined, $z = z(m_0, C)$.

We detail the method used by the Stony Brook group (Lanzetta et al. 1996; Fernàndez-Soto et al. 1999) to give some flavor of photometric redshift determinations. They begin with the four empirical galaxy spectral energy distributions of Coleman, Wu, & Weedman (1980), corresponding to four observed galaxy types (E/S0, Sbc, Scd, and Irr) and covering the wavelength range $1400 - 10,000$ Å. The templates are extrapolated in the UV to 912 Å using the empirical spectra of Kinney et al. (1993), and are extrapolated in the infrared to 25 μm using the spectral evolutionary models of Bruzual & Charlot (1993). The hybrid templates are redshifted and the redshift-dependent ultraviolet hydrogen absorptions are removed using a model of the optical depth of hydrogen. At modest redshift, this transmission function is empirically derived from observations of quasars (e.g., Madau 1995). The shifted, absorbed spectra are then convolved with the transmission curves of the relevant filters and a redshift likelihood function is calculated relating the model colors to measured fluxes. Comparisons between photometric and spectroscopic redshift determinations in

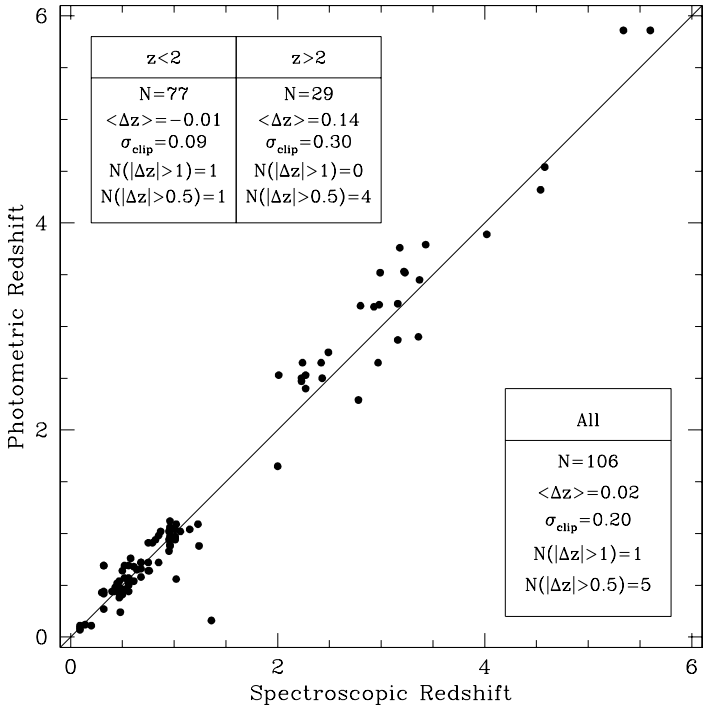

Fig. 7.— A comparison of spectroscopic and photometric redshifts in the (Northern) HDF. Photometric redshifts are from the Stony Brook group, as detailed in the text. Spectroscopic redshifts are from the literature. Insets indicate various comparisons between the redshift determinations in two redshift bins as well as the entire sample: N is the number of galaxies, $\langle \Delta z \rangle$ is the average difference between $z_{\rm spec}$ and $z_{\rm phot}$, $\sigma_{\rm clip}$ is the clipped dispersion between the measurements, and $N(|\Delta z| > 0.5, 1)$ measures the number of outlier photometric redshift determinations. Although this plot reports solely on the Stony Brook photometric redshift determinations, dispersions of $\sigma \approx 0.2$ between $z_{\rm spec}$ and $z_{\rm phot}$ are typical of many of the successful photometric redshift measurements in the HDF. Figure courtesy Fernàndez-Soto.

the HDF show that the former is typically robust to $\Delta z \approx 0.34$ for objects with $I_{814} \sim 25.5$ and $z > 3$. Residuals are typically $\Delta z_{\rm rms}/(1+z) \approx 0.1$ at all redshifts (see Fig. 7).

Other template photometric redshift estimates generally vary in only two considerations: (1) the input spectral templates and (2) the method of determining the best-fit $z_{\rm phot}$. Input spectral templates may be purely empirical, purely synthetic, or hybrid as in the Stony Brook analysis (see Table 3). Input libraries may also vary in the number of templates. Many groups use the four empirical spectral energy distributions of Coleman et al. (1980). The addition of one or more star-forming galaxy templates, as assembled by Calzetti, Kinney, & Storchi-Bergmann (1994), has been noted to improve the accuracy of the photometric redshift determination by some groups. Determination of the best-fit $z_{\rm phot}$ relies on a statistical analysis. For example, the Stony Brook group uses a maximum likelihood analysis, while Benítez (1999) applies Bayesian marginalization and prior probabilities to the problem.

The training set method has the advantage of being purely empirical, and therefore not relying on a choice of input templates. However, the weakness is that the method requires and is dependent upon a large and accurate input training set. Redshift ranges with sparse numbers of confirmed redshifts, such as $1 \lesssim z \lesssim 2.5$ and $z \gtrsim 4$, lead to poorly determined photometric redshift determinations. The various practitioners of this technique vary in the degree polynomial used to fit the multivariate function $z = z(m_0, C)$ and whether or not they implement observed flux as a variable in the optimal fit.

In terms of the current review on search techniques for protogalaxies, we are most interested in the robustness of these photometric procedures in identifying the high-redshift ($z \gtrsim 4$) tail in the field galaxy redshift distribution. Fernàndez-Soto et al. (1999) find 5 galaxies brighter than $I_{814} = 26.5$ in the HDF with $4.5 < z < 5.5$, corresponding to a surface density of 1.0 galaxies per square arcminute per unit z at $z = 5$. Spectroscopic confirmation of the high-redshift photometric candidates is necessary to validate the technique before photometric redshift measurements of, for example, the star-formation history of the early Universe, are well established. Over the past three years, our Berkeley-based group has been using slitmasks with the Low Resolution Imaging Spectrometer (LRIS; Oke et al. 1995) on the Keck II telescope to measure faint galaxy spectra in the HDF. We choose $z \gtrsim 4$ candidates in collaboration with the Stony Brook-based photometric redshift group. With the current instrumentation, spectroscopic redshift measurements are viable perhaps to $I_{814} \approx 27.5$ for emission line sources and to $I_{814} \approx 26$ for objects without strong emission lines. But even at $I_{814} \approx 25.5$, the effort is fairly "heroic": observations of a single faint galaxy can easily extend over multiple observing seasons in order to measure a reliable spectroscopic redshift. Fig. 8 presents Keck/LRIS spectra of three high-redshift sources in the HDF obtained by our Berkeley-based group. In Table 4 we list a comparison of spectroscopic and photometric redshifts for galaxies in the HDF at $z > 4$.

Table 4: Spectroscopic vs. Photometric Redshifts in the HDF at $z > 4$

Galaxy	$z_{\rm spec}$	$z_{\rm phot}$	$W_{\rm Ly\alpha}^{\rm obs}$ (Å)	I_{814} (AB) (mag.)	Reference
HDF 3−512.0	4.02	3.56	$\gtrsim 200$	25.5	Dickinson (1998)
HDF 4−439.0	4.54	4.32	~ 20	24.9	Stern et al. (2000)
HDF 4−625.0	4.58	4.52	~ 100	25.2	Stern et al. (2000)
HDF 3−951.0	5.33	5.72	$\cdots$	25.6	Spinrad et al. (1998)
HDF 4−473.0	5.60	5.64	~ 300	27.1	Weymann et al. (1998)

Notes.— Photometric redshift $z_{\rm phot}$ from Fernàndez-Soto et al. (1999). I_{814} magnitude from Williams et al. (1996).

The reliability of the photometric redshifts in the $4 \lesssim z \lesssim 5$ regime seems excellent. Even at lower redshifts, only $\approx 5\%$ of the photometric redshifts are noticeably discordant when compared to spectroscopic redshifts. However, looking ahead, as we push the frontier past $z = 6$, the hydrogen absorptions are predicted to almost completely obliterate the observed optical flux. Deep near-infrared photometry will be necessary, observations which are best done from space, above the

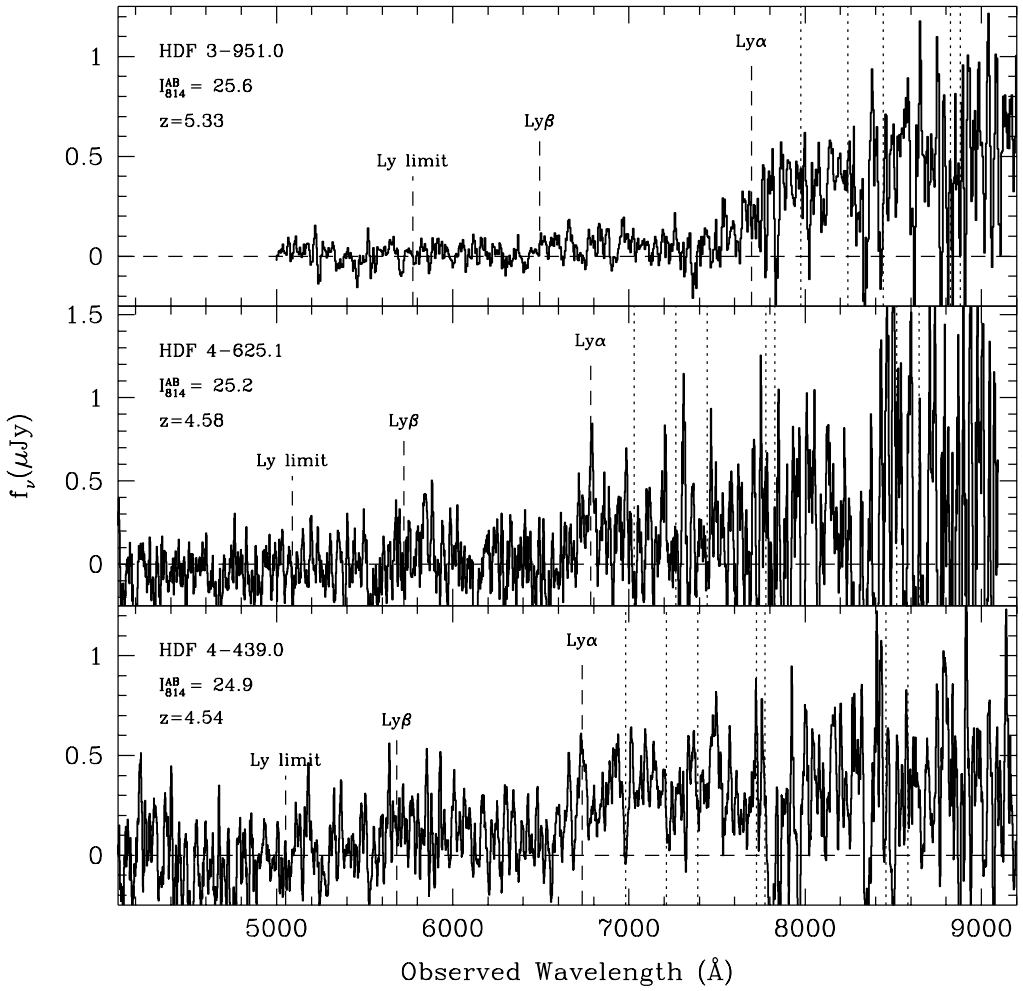

Fig. 8.— Keck/LRIS spectra of HDF 3-951.0, HDF 4-625.0, and HDF 4-439.0, three photometrically-selected high-redshift galaxies in the HDF. The spectrum of HDF 3-951.0 represents 6 hours of integration with the 150/7500 lines mm^{-1} grating, significantly more sensitive than the discovery spectrogram presented in Spinrad et al. (1998). The slightly-revised redshift of $z = 5.33$ is based on the Lyβ discontinuity, which is located at a wavelength less affected by telluric emission than the Lyα discontinuity. The spectra of HDF 4-625.0 and HDF 4-439.0 represent sums of data from multiple observing seasons. Vertical dotted lines indicate the location of absorption lines typically observed in Lyman-break galaxies at $z \simeq 3$.

atmospheric water absorptions. The NICMOS camera on the *Hubble Space Telescope* (*HST*) has left a valuable legacy of data and the Next Generation Space Telescope (*NGST*) is being planned to work long-ward of 1μm.

4.3. Emission Lines Searches for Distant Galaxies

The stellar population synthesis models of Charlot & Fall (1993) predict rest-frame Lyα equivalent widths of $50 - 200$ Å for young, dust-free galaxies. An unattenuated Lyα equivalent width of 200 Å corresponds to $\approx 5\%$ of the bolometric luminosity of the protogalaxy being emitted as Lyα photons. For a constant star formation history, the Lyα luminosity and equivalent width are only somewhat dependent on the star formation rate and are greatest at times less than 10 Myr after the onset of the burst. Although this line emission is quite vulnerable to extinction from dust, little dust might be expected in the first phase of star formation. Indeed, Thommes et al. (1998) suggest requiring strong Lyα emission as a necessary criterion for primeval galaxies. Alternatively, dust production can proceed remarkably quickly in supernovae remnants, implying that most "primordial" galaxies may contain substantial dust by the time we observe them. We note that recent ultraviolet studies of low-redshift Lyα suggest that the kinematics of neutral gas may be the more important attenuator of line emission ( )]Kunth:98a.

Several programs are currently underway to search for high-redshift primeval galaxies through deep narrow-band imaging. The previous generation of surveys failed to confirm any field Lyα-emitting protogalaxy candidates (Thompson & Djorgovski 1995; Pritchet 1994). One of the new programs is the Calar Alto Deep Image Survey (CADIS; Thommes et al. 1998) which uses a Fabry-Pérot interferometer to search for emission lines in three windows of low night sky emission corresponding to Lyα at $z = 4.75$, 5.75, and 6.55. The survey will eventually sample 0.3 deg^2 of sky to a flux density limit of $S_{\rm lim}(5\sigma) \approx 5 \times 10^{-17}\,{\rm ergs\,cm^{-2}\,s^{-1}}$. The technique employs an arsenal of narrow-band 'veto' filters to distinguish foreground emission-line galaxies from distant Lyα emitters. Medium-band filters are also used to discriminate foreground objects from Lyα-emitting protogalaxy candidates at high redshift on the basis of spectral energy distributions. Six early candidates were reported in Thommes et al. (1998). However, follow-up spectroscopy with the Keck II telescope has not confirmed a Lyα interpretation for any of these sources; Thommes (1999) present a revised candidate surface density of 0.2 Lyα emitters per square arcminute per unit-z at $z = 5.75$ to the relatively-bright CADIS survey flux-density limit.

Another program to identify strong Lyα-emitting star-forming galaxies recently has been started at the Keck II telescope (Cowie & Hu 1998; Hu et al. 1998). Using a combination of narrow-band interference filter imaging and broad-band imaging, they discriminate high-redshift Lyα emitters on the basis of high equivalent width ($W_\lambda^{\rm obs} > 77$ Å) and broad-band color. The survey probes to a flux density limit of $S_{\rm lim}(5\sigma) \approx 1.5 \times 10^{-17}\,{\rm ergs\,cm^{-2}\,s^{-1}}$. Preliminary results, covering 46 arcmin^2 with a 5390/77 Å filter, suggest a surface density of ≈ 3 Lyα emitters per square arcminute per unit-z at $z \sim 3.4$ (Cowie & Hu 1998). The Hawaii group has narrow-band filters tuned to gaps in the telluric OH emission, corresponding to redshifts $z = 3.4, 4.5, 5.8$ and 6.5.

Serendipitous searches on deep slit spectra, as discussed in the following subsection (§4.4), are also sensitive to line emission. A technique combining narrow-band filters and spectroscopy is

discussed in §4.5.

Of course, identification of a strong emission line alone does not necessarily imply the detection of high-redshift Lyα. Arguments based upon the equivalent width of the line, lack of other emission lines, the line profile, and associated continuum decrements are typically used to determine the line identity (e.g., Stern et al. 1999a). However, selecting objects on the basis of strong emission samples a different galaxy population from the traditional magnitude-limited surveys: emission-line surveys are much more sensitive to active galaxies and objects undergoing massive bursts of star formation. Distinguishing the redshift and source of line emission is challenging; comparison to field surveys selected on the basis of continuum magnitude is perhaps inappropriate.

For example, Stern et al. (1999a) recently reported the serendipitous detection of an emission line at 9185 Å with an observed frame equivalent width > 1225 Å (95% confidence limit). The spectral atlas of nearby galaxies by Kennicutt (1992) shows that the rest-frame equivalent width of the Hα + [N II] complex rarely exceeds 200 Å, that of [O III]λ 5007 Å rarely exceeds 100 Å, Hβ rarely exceeds 30 Å, and [O II]λ 3727 Å (hereinafter [O II]) rarely exceeds 100 Å. Field surveys of moderate-redshift, star-forming galaxies substantiate that [O II] rarely has a rest-frame equivalent width exceeding 100 Å (e.g., Songaila et al. 1994; Guzmàn et al. 1997; Hammer et al. 1997; Hogg et al. 1998). Preliminary analysis would strongly suggest that this source was a Lyα-emitter at $z = 6.56$, for which the implied rest-frame Lyα equivalent width would be consistent with confirmed sources at $z > 5$ (Dey et al. 1998; Weymann et al. 1998). However, a long exposure Keck/LRIS spectrogram revealed a source $2\farcs7$ away with strong [O II] emission offset by only 7 Å spectrally, persuasively arguing that this is an unusual, likely active, [O II]-emitting system at $z = 1.46$.

Infrared programs, similar to these optical programs, have begun to yield some candidates, most likely at intermediate redshift thus far. Malkan, Teplitz, & McLean (1995) and Teplitz, Malkan, & McLean (1998), using the NIRC camera on the Keck I telescope, detect Hα (but possibly [O II] or [O III]) emission using the 2.16μm narrow-band CO filter. These initial searches were targeted; i.e., fields were selected to search for spatially-correlated emission line galaxies around known quasars or damped quasar absorption systems.

McCarthy et al. (1999) report on blank-sky grism searches obtained during parallel time with the NICMOS camera on *HST*. The observations sample $\approx 1.1 - 1.9\mu$m and are unaffected by atmospheric water absorption bands. They find a surface density of single emission line galaxies (most likely Hα) of ≈ 0.5 galaxies per square arcminute to a limiting flux density of 2×10^{-17} ergs cm^{-2} s^{-1}. No variation with wavelength (redshift) is statistically significant in their data set, which corresponds to Hα emission over the redshift range $0.7 \lesssim z \lesssim 1.9$. Recombination theory coupled with an assumed stellar luminosity function can be used to relate Hα luminosity to the star-formation rate $\dot{M}$ (e.g., Kennicutt 1983; Madau, Pozzetti, & Dickinson 1998). Yan et al. (1999) find an average star-formation rate of $\dot{M} = 21\ h_{50}^{-2}\ M_\odot\ \mathrm{yr}^{-1}$.

Fig. 9.— See fig9.jpg.Two-dimensional spectrogram of serendipitously-discovered strong line emitters in the SSA22 field. The source SSA22-C17 is a Lyman-break galaxy at $z = 3.299$ discovered by Steidel and collaborators. During deep, moderate-dispersion Keck/LRIS follow-up spectroscopy of that source, two strong line-emitters were serendipitously discovered on the same multislit slitlet. The high-equivalent widths, lack of secondary emission features, and narrow velocity width of the lines argue that these are high-redshift Lyα-emitters. Figure courtesy Manning et al. (2000).

4.4. Serendipitous Longslit Searches

Deep spectroscopy alone is also an efficient means to detect Lyα emission from very high-redshift systems (see Fig. 9). Long spectroscopic integrations are sensitive to line-emitting sources which serendipitously fall within the slit, potentially out to $z \approx 6.5$. This limit is set by the plummetting response of CCDs in the near-infrared and to some degree by the strong OH sky emissions at $\lambda > 9300$ Å; infrared spectrographs can potentially extend these surveys to still higher redshifts. The first confirmed object at $z > 5$ was the result of a serendipitous detection ( );][]Dey:98. Hu et al. (1998) also report the serendipitous detection of an isolated emission line source which they interpret as Lyα at $z > 5$. Serendipitous longslit searches are fully complementary to narrow-band work: whereas narrow-band imaging probes a thin shell of redshift space, deep spectroscopy (admittedly over a smaller solid angle) probes a pencil beam of look-back time. The resolution of low-dispersion optical spectrographs are also better matched to typical Lyα line widths than filters with widths of 3000 $\mathrm{km\,s^{-1}}$.

At Berkeley, we are conducting a careful analysis of our deepest archival spectroscopic exposures on the Keck telescopes obtained in good meteorological conditions (see Fig. 9). In a 1.5 hour spectrogram at moderate-dispersion ($\lambda/\Delta\lambda \simeq 1000$) with the LRIS camera, the limiting flux density probed for spectrally unresolved line emission in a 1 arcsec^2 aperture is $S_{\rm lim}(5\sigma) \approx 1 \times 10^{-17}\,\mathrm{ergs\,cm^{-2}\,s^{-1}}$ at $\lambda \approx 9300$ Å (Stern et al. 1999a). The limit is strongly wavelength dependent. A single slitmask exposure typically covers ≈ 600 square arcseconds, or one-sixth of a square arcminute. In a year, up to $\gtrsim 2$ square arcminutes can be covered, implying reasonable statistics on the surface density of high-redshift line emitters, only somewhat compromised when portions of the mask are dedicated to photometric high-redshift candidates or when observations target rich clusters. This work is in progress (Manning et al. 2000) and the reader will appreciate that distinguishing Lyα serendips from lower-redshift interlopers can be challenging and is best done with follow-up spectroscopic and/or deep multi-band imaging observations. Our observations typically are biased towards redder wavelengths, which has the unfortunate consequence that we are not sensitive to $z \sim 3$ serendips and thus cannot compare our results to well-documented results of Steidel and collaborators at that redshift interval (e.g., Steidel et al. 1996a, 1996b; Dickinson 1998; Steidel et al. 1999). We are currently emphasizing serendipitous Lyα-emitting galaxies at $4.5 \lesssim z \lesssim 5.5$. We have four reasonable candidates in the ≈ 1.6 square arcminutes analyzed thus far, not including candidates behind the Abell 2390 cluster. One source is confirmed at $z = 5.34$

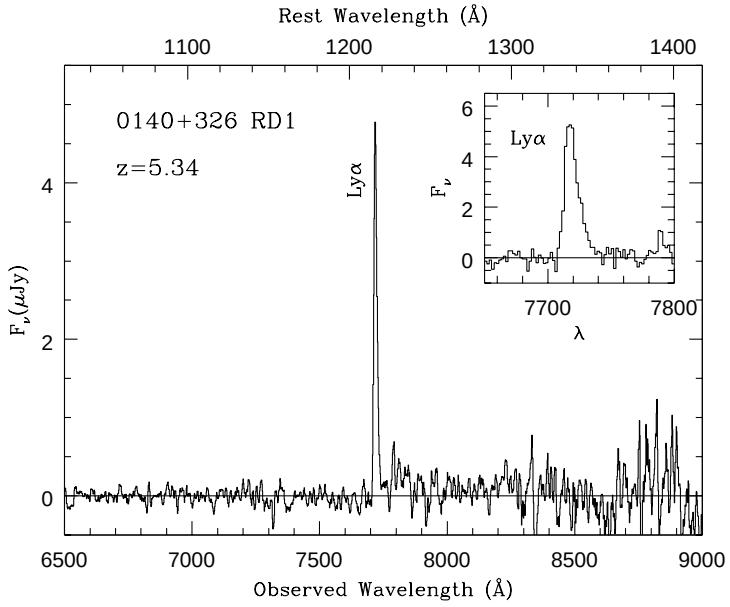

Fig. 10.— Co-averaged spectrum of the serendipitously discovered galaxy 0140+326 RD1 at $z = 5.34$ ($I = 26.1$; Dey et al. 1998). The total exposure time is 36.2 ksec. Note the strong Lyα emission and the continuum discontinuity short-ward of the line which confirms the redshift identification. The 'features' observed in the continuum are largely due to residuals from the subtraction of strong telluric OH emission lines (e.g., 8344 Å). The inset shows the asymmetric profile of the Lyα emission line. Figure courtesy Dey et al. (1998).

(Dey et al. 1998). We also have a few candidates at $z > 5.5$ which are not included in the current discussion. The measured surface density is $\approx 2 \pm 1$ candidate Lyα emitters per square arcminute at $z = 5$. Their continua are estimated to be quite faint, $I \gtrsim 26.5$ (AB). Serendipitously-identified absorption-break galaxies at high redshift are also possible, but difficult at the faint levels we now probe.

4.5. Narrow-band Spectroscopy

An additional hybrid method, combining elements of both the narrow-band imaging and serendipitous longslit search techniques, involves obtaining many limited-wavelength spectra through a medium-width (OH-avoidance) filter (e.g., Crampton 2000). With a uniform placement of thirty $2''$ wide, $9'$ long parallel slitlets, Crampton (2000), using the Canada-France-Hawaii Telescope atop Mauna Kea, probes 9 square arcminutes of sky per mask observation with a narrow-band filter plus low dispersion grism. The survey is designed to search for Lyα at $6.38 < z < 6.64$, corresponding to a region of both low OH emission and low H_20 absorption. This hybrid approach has the advantage of providing spectra of all targets over a short wavelength region. This is important for distinguishing high-redshift Lyα, which can be identified both by line profile and by the presence

of a strong continuum decrement across the line. Lower-redshift emission features might also be identified from the presence of secondary lines, such as [O III]λ 4959 Å near [O III]λ 5007 Å, or the double profile of [O II]$\lambda\lambda$ 3727,3729 Å. Finally, as mentioned in §4.4, the higher resolution of spectroscopy relative to narrow-band imaging is more sensitive to the typical emission line widths, making this hybrid approach an efficient method for probing the distant Universe.

4.6. Targeted Searches

Finally, we briefly mention some targeted programs to identify high-redshift galaxies associated with distant quasars. A handful of galaxies within a few arcseconds of distant quasars have been identified at redshifts corresponding to damped Lyα absorptions in the quasar spectra (e.g., Djorgovski et al. 1996). Searching for galactic companions to distant quasars has also proved successful. Djorgovski et al. (1985) report on an emission-line-selected source with a probable redshift of $z = 3.218$ associated with the quasar PKS 1614−051 at $z = 3.209$. More recent programs have used combinations of narrow-band imaging and photometric color selection to search for quasar companions at $z > 4$. Several teams have identified companions to BR 1202−0725 at $z = 4.695$ (Djorgovski 1995; Hu et al. 1996; Petitjean et al. 1996). Hu & McMahon (1996) report on two companions to BR 2237−0607 at $z = 4.55$. Djorgovski et al. (2000) presents a status report of an on-going program to search for protoclusters around ≈ 20 quasars at $z > 4$. Preliminary results imply co-moving number densities of protogalaxies two to four orders of magnitude higher than expected for the field. These results support biased galaxy formation models, in which galaxies preferentially form in the densest peaks of the primordial density field.

4.7. Summary

In Table 5 we summarize the surface densities measured (estimated) from the various search techniques described above. We see that the non-optical search techniques have very low surface densities, most spectacularly for GRBs whose surface density is $\lesssim 10$ per year per Hubble volume. The optical/near-IR techniques which are sensitive to normal, star-forming galaxies, typically have surface densities of a few per square arcminute per unit redshift. In §6 we consider the biases in the different techniques and discuss how independent the methods may be.

5. "Protogalaxies" at Low-Redshift

The above discussion has focussed on identifying young galaxies at the highest accessible redshifts. The observed optical emission then necessarily samples the rest-frame ultraviolet. However, galaxy formation is an ongoing process; locally we see several galaxies with metallicities close to primordial (Kunth et al. 1994; Thuan & Izotov 1997). These nearby young systems sample a

Table 5: Surface Densities of High-Redshift Galaxies

Technique	z range	# / sq. arcmin	Limiting Flux Density	Reference
radio sources	all z	≈ 0.03	$S_{1.4\mathrm{GHz}} > 1$ mJy	1
sub-mm galaxies	all z	≈ 0.09	$S_{850\mu\mathrm{m}} > 2$ mJy	2
X-ray sources	all z	0.27 ± 0.04	$10^{-15}\,\mathrm{ergs\,cm^{-2}\,s^{-1}}$	3
GRBs	all z	$\approx 10^{-7}$ / yr	...	...
Lyman-break galaxies	$z \sim 3$	0.68 ± 0.02	$R^{\mathrm{AB}} \leq 25.0$	4
Lyman-break galaxies	$z \sim 4$	0.21 ± 0.02	$I^{\mathrm{AB}} \leq 25.0$	4
photometric candidates	$4.5 - 5.5$	≈ 1.0 / unit-z	$I^{\mathrm{AB}}_{814} \leq 26.5$	5
narrow-band surveys, CADIS	$z \sim 5.75$	0.2 / unit-z	$5.0 \times 10^{-17}\,\mathrm{ergs\,cm^{-2}\,s^{-1}}$ (5σ)	6
narrow-band surveys, Hawaii	$z \sim 4.6$	≈ 3 / unit-z	$1.5 \times 10^{-17}\,\mathrm{ergs\,cm^{-2}\,s^{-1}}$ (5σ)	7
grism survey, NICMOS	$0.7 - 1.9$	0.5	$2.0 \times 10^{-17}\,\mathrm{ergs\,cm^{-2}\,s^{-1}}$	8
serendip survey, Berkeley	$4.5 - 5.5$	$\approx 2 \pm 1$ / unit-z	$1.0 \times 10^{-17}\,\mathrm{ergs\,cm^{-2}\,s^{-1}}$ (5σ)	9

Notes.— References: (1) Becker et al. (1995); (2) Hughes et al. (1998); (3) Hasinger et al. (1998); (4) Steidel et al. (1999); (5) Fernàndez-Soto et al. (1999); (6) Thommes et al. (1998); (7) Cowie & Hu (1998).; (8) McCarthy et al. (1999); (9) Stern et al. (1999a).

different segment of the galaxy luminosity function from the high-redshift systems discussed above — the expectation is that high-redshift galaxies are the progenitors of present-day massive galaxies (L^* systems and larger) while the local low-metallicity systems are all very low-mass dwarf galaxies. Nevertheless, high-signal-to-noise ultraviolet observations of the local protogalaxy population provide a very useful laboratory for studying and understanding the high-redshift population.

As mentioned earlier, models predict strong ($50 - 200$ Å equivalent width) Lyα emission from young, dust-free galaxies forming their first generation of stars (e.g., Charlot & Fall 1993). However, *International Ultraviolet Explorer* (*IUE*) observations of local star-forming galaxies revealed Lyα strengths considerably weaker than predicted by case B recombination: the Lyα/Hβ intensity ratio was always found to be $\lesssim 10$, as opposed to the theoretical value of 33. Furthermore, some galaxies showed Lyα absorbtion rather than emission. Small amounts of dust intermixed with the extended neutral gas was the assumed culprit (e.g., Hartmann, Huchra, & Geller 1984). Hartmann et al. (1988) showed evidence for an anti-correlation of Lyα strength with metallicity, which conformed to a simplistic scheme of chemical enhancement and motivated searches for strong Lyα emission in distant galaxies with anticipated primordial abundances. More recently, *HST* observations of the two most metal-deficient galaxies known, I Zw 18 ($Z = Z_\odot/51$; Kunth et al. 1994) and SBS 0335−052 ($Z = Z_\odot/40$; Thuan & Izotov 1997) show Lyα in *absorption* rather than emission, at odds with the results of Hartmann et al. (1988).

Kunth et al. (1998) present *HST* ultraviolet spectra of eight H II galaxies covering a wide range of metallicity. The observations were designed to cover both the Lyα region and the region around O I λ1302 Å and Si II λ1304 Å. The former region allows study of the Lyα emission and absorption properties and an estimate of the H I column, while the latter allows a crude estimate of the chemical composition of the gas and a measure of the velocity of the gas with respect to

the systemic velocity of the system as measured from optical emission lines. Surprisingly, they find that the primary indicator of Lyα strength is kinematics, not metallicity. The four systems with metallic lines static with respect to the ionized gas show damped Lyα absorption, while the four systems with Lyα emission show the metallic lines blueshifted by ≈ 200 km s^{-1} with respect to the ionized gas. The implications are that even nearly primordial clouds undergoing star formation have sufficient dust columns to suppress Lyα emission provided the kinematics of the neutral gas allows resonant scattering of the Lyα emission. In all cases reporting Lyα emission in the Kunth et al. (1998) sample, an asymmetric profile with a sharp blue cutoff is observed.

In addition to the local star-forming galaxies with (1) broad, damped Lyα absorption centered at the wavelength corresponding to the redshift of the H II gas and (2) galaxies with Lyα emission marked by blueshifted absorption features, Kunth et al. (1999) notes a third morphology of Lyα line that is occasionally observed in the local Universe: (3) galaxies showing 'pure' Lyα emission, i.e., galaxies which show no Lyα absorption whatsoever and have symmetric Lyα emission profiles. Terlevich et al. (1993) presents *IUE* spectra of two examples: C0840+1201 and T1247−232, both of which are extremely low-metallicity H II galaxies. Thuan, Izotov, & Lipovetsky (1997) present a high signal-to-noise ratio *HST* spectrum of the latter galaxy, noting that with $Z = Z_{\odot}/23$, it is the lowest metallicity local star-forming galaxy showing Lyα in emission. At higher signal-to-noise ratio and higher dispersion than the *IUE* spectrum, the line shows multiple absorption features near the redshift of the emission, bringing into question the 'pure' designation. Tenorio-Tagle et al. (1999) have proposed a scenario to explain the variety of Lyα profiles based on the hydrodynamical evolution of superbubbles powered by massive starbursts.

This scenario and observations of local star-forming galaxies have two important implications for studies of high-redshift protogalaxies. First, they provide a natural explanation for asymmetric profiles which seem to characterize high-redshift Lyα (e.g., see Fig. 10), but also imply that although the asymmetric profile may be a sufficient condition for identification of a strong line with Lyα, it is not a necessary condition. This point is particularly important for judging the identification of serendipitous and narrow-band survey emission sources whose spectra are dominated by a solitary, high equivalent width emission line. Second, if Lyα emission is primarily a function of kinematics and perhaps evolutionary phase of a starburst, attempts to derive the co-moving star-formation rate at high redshifts from Lyα emission will require substantial and uncertain assumptions regarding the relation of observed Lyα properties to the intrinsic star formation rate; use of the UV continuum ($\lambda \approx 1500$ Å) may be preferred for measuring star formation rates.

6. Biases in Distant Galaxy Search Techniques

We now consider the biases which affect the various galaxy search techniques discussed in §3 and §4. Each technique provides a shaded view of the deep extragalactic Universe; we enumerate these differences in the same order that the various techniques were presented.

Radio galaxies are classical AGN. This implies, according to the prevailing models of active galaxies, the presence of a supermassive black hole. Nearby radio galaxies are associated with large early-type galaxies, both cDs in the centers of clusters and giant elliptical galaxies. Conventional wisdom states that HzRGs are the precursors to these early-type systems; our bias may simply be that HzRGs sample the most massive systems. At the least, though, HzRGs necessitate the presence of a supermassive black hole in the early Universe. The time scale of supermassive black hole formation is not well-known (e.g., Loeb 1993). Are black holes the seeds of early galaxy formation, or are they the fruit of it? The radio source itself most likely affects the assembly of the galactic sub-units, triggering star-formation along the radio jets in at least some cases (e.g., Dey et al. 1997). If HzRGs are indeed found to be the precursors of the most massive early-type systems, radio galaxies at high redshift may prove to be most important for studies of the formation of galaxy clusters and large scale structure.

Sub-mm and infrared-selected (LIRG) sources require much of their bolometric luminosity to be dust-reprocessed radiation emitted at long wavelength. In an extreme scenario, one could imagine a dust-enshrouded starburst in which no radiation short-ward of a few microns escaped a restricted spatial region. Such a source at high redshift would escape detection in contemporary optical/near-infrared surveys; it would perhaps only be detected in the 850μm sub-mm region. Have any such sources been identified already? Astrometric uncertainties and the large beam-size of the SCUBA detector leave the question open. It is conceivable that one or more of the Hughes et al. (1998) sub-mm sources in the HDF lack optical/near-infrared identifications, even to the extremely deep limits of the HDF. Though studies of field sub-mm sources are in their nascent phases, it is likely these systems represent those galaxies in the distant Universe undergoing the most vigorous bursts of star formation. We are far from the time when we can reliably relate these distant sources to the local census of galaxies, but conceiving of the sub-mm population as the more distant cousins of ultraluminous infrared galaxies (ULIRGs) seems plausible, if not likely (e.g., Lilly et al. 1999). At the least, sub-mm galaxies are important as they produce a significant fraction ($\geq 15\%$) of the total bolometric output of the Universe averaged over all wavelengths and epochs (Lilly et al. 1999) and largely (entirely?) account for the sub-mm background. Sub-mm galaxies may be the precursors of metal-rich spheroids.

X-ray selection of distant sources likely necessitates the presence of an AGN, implying that studies of the most distant X-ray sources may be most important for understanding the formation of supermassive black holes. Extended cluster X-ray sources derive from the thermal brehmsstrahlung in hot, ionized intercluster media. Galaxy clusters sample the deepest potential wells in the Universe on Mpc scales. Studies of the most distant X-ray clusters will provide valuable information on the formation of large-scale structure. In particular, several authors have noted the sharp dependence of the evolution of cluster abundances on basic cosmological parameters (e.g., Eke et al. 1996).

The first optical identification of a GRB occurred less than two years ago, and our understanding of these intriguing sources, though much improved, is still rather sparse. Are GRBs more prevalent in young stellar systems with many massive remnants? Are they correlated with SNe

explosions? It is premature to comment too deeply on what biases GRB-selected host galaxies may yield on our understanding of the distant Universe. At the least, they are not *all* heavily reddened, which has implications for the prevalence of dust in the Universe.

Lyman-break galaxies and photometrically-selected young galaxies at high redshift are biased against dusty systems and older populations which would redden the observed spectral energy distributions and likely lead to redshift ambiguities. The main bias is that these techniques only search for galaxies containing a very young, OB star-rich, stellar population which dominates the rest-frame continuum in the wavelength range $\lambda\lambda 1216 - 1700$ Å. A small contribution by an older population of stars will not be very noticeable at the observed, deep-ultraviolet wavelengths available for study at high redshift. Near-infrared studies with spectrographs on the new generation of 9 ± 1 m telescopes, and later from NGST, will provide critical information on the masses, kinematics, ages, and dust abundance in this population. Are we only skimming the envelope of the most dust-poor young systems? The relation of the Lyman-break galaxies to the local galaxy population remains uncertain.

Lyα searches for distant galaxies have a clear, but uncertain, observational bias; strong Lyα emission ($W_\lambda > 20$ Å) tends to be biased against dusty galaxies, or at least against galaxies whose neutral gas has unfavorable geometry/kinematics. Spectroscopy of the Lyman-break population reveals that approximately half of the galaxies show Lyα in *absorption*. In fact, deep narrow-band imaging compared to broad-band images can show these systems as negative holes (Steidel 2000)! However, most astronomers involved in Lyα surveys are restricting their search to emission-line sources. The surface densities measured (see Table 5) are comparable to those measured for Lyman-break galaxies. The implication is that a large population of strong Lyα emitters exist which have fainter continua than the limits of the photometric surveys. If the morphology of the Lyα emission primarily depends upon the kinematics of the neutral gas as suggested by ultraviolet studies of local metal-poor galaxies (§5), then caution should be advised in deriving star formation rates and densities from the Lyα-emitting galaxies.

7. Results: First Glimpses towards the Dark Ages

Observational study of normal galaxies at $z \gtrsim 3$ is still a rather recent phenomenon. The last invited review on the subject to this journal, only five years past (Pritchet 1994), began with the sad pronouncement that the predicted widespread population of primeval galaxies had thus far escaped detection. At the time, our knowledge of individual sources at $z > 3$ was restricted to a dozen or so radio galaxies and a larger census of quasars. Now the pioneering work of Steidel and collaborators has uncovered several hundreds of Lyman-break systems at $z \gtrsim 3$ and spectroscopically confirmed galaxies have recently crossed the $z = 5$ barrier. Studies of the earliest epochs of the Universe are no longer restricted to AGN and quasar enthusiasts: since 1997 December (Franx et al. 1997) the most distant sources known to astronomers have consistently been apparently normal, star-forming galaxies. Though this review emphasizes the search techniques for identifying distant galaxies, we

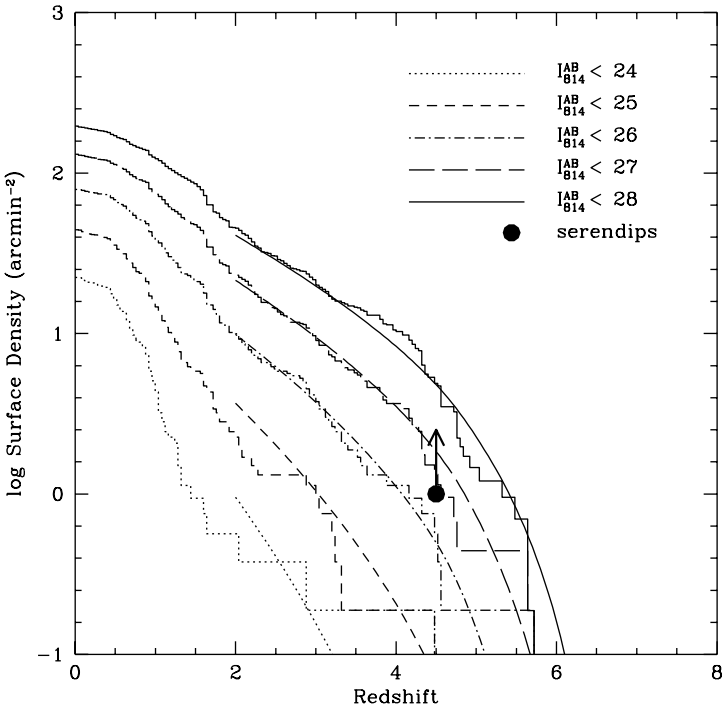

Fig. 11.— Cumulative surface density of galaxies as a function of redshift and limiting $I_{814}^{\rm AB}$ magnitude. Histograms are Stony Brook photometric redshift measurements of the cumulative surface density of galaxies in the (Northern) HDF. Curves are fits to the histograms assuming a parametrization of the evolving galaxy luminosity function (see text). The point at $z = 4.5$ indicates our estimate of the lower limit to the observed surface density of high-redshift serendipitous Lyα-emitters ($S_{{\rm Ly}\alpha} \simeq 1.0 \times 10^{-17}\,{\rm ergs\,cm^{-2}\,s^{-1}}$, 5 σ). Figure courtesy Lanzetta (2000).

now briefly consider what has been and can be learned about the early Universe from these studies.

7.1. Surface Densities of High-Redshift Galaxies

Our various types of distant galaxies may be illustrative of peculiar, rare denizens of the cosmic past (the few powerful steep-spectrum radio sources at $z > 4$) or they may be more modest star-forming citizens, representative of an era when normal galaxies were modest fractions of L^* and M^*, typical luminosities and masses of the current cosmic epoch near $z = 0$.

In Table 5 we summarized the measured (estimated) surface densities of the various classes of distant sources discussed. Of particular note are the optical/near-infrared selected sources which present our best hope at being identified with precursors of present-day typical galaxies.

Fig. 11 illustrates the cumulative galaxy surface density as a function of redshift and $I_{814}^{\rm AB}$

magnitude — i.e., the surface density of galaxies of redshift greater than a given redshift for different magnitude thresholds. For example, to a limiting magnitude of $I_{814}^{\rm AB} = 26$, ≈ 5 galaxies per square arcminute are expected at $z > 3$. The histograms derive from Stony Brook photometric redshift measurements in the (Northern) HDF. The curves are fits to the measurements, assuming that the evolving galaxy luminosity function is parameterized by the Schechter (1976) luminosity function,

$$\phi(L)dL = \phi^*(L/L^*)^\alpha \exp(-L/L^*)d(L/L^*), \tag{1}$$

where $\phi(L)$ is the number density of galaxies per unit comoving volume and the characteristic galaxy luminosity at rest-frame 1500 Å $L_{*,1500}$ evolves with redshift as

$$L_{*,1500} = L_{*,1500}^{z=3}(1+z)^\beta. \tag{2}$$

Lanzetta (2000) finds that the photometric redshifts are best fit with a characteristic absolute magnitude at 1500 Å $M_{*,1500}^{z=3} = -19.5 \pm 0.5$, a moderately steep luminosity function $\alpha = -1.43 \pm 0.05$, and an evolving characteristic luminosity where $\beta = -0.7 \pm 0.4$. Also plotted in Fig. 11 is our estimated lower limit to the surface density of serendipitous sources at $z > 4.5$ from longslit searches (> 1 arcmin^{-2}).

Substantial caveats regarding this plot should be kept in mind before extragalactic astronomers halt spectroscopic redshift surveys. First, the modest angular size of the HDF implies that substantial cosmic variance may skew the results, particularly at the brightest absolute magnitudes for each redshift interval. Gwyn (2000) notes significant differences in the distribution of photometric redshifts between the HDF-N and the HDF-S. Similarly, since the HDF samples a very small volume of the local Universe, the low-redshift surface densities are poorly determined. Second, the redshifts are based on photometric determinations rather than spectroscopic determinations. As shown in §4.2, photometric measurements are fairly robust at the magnitude and redshift ranges tested thus far. However, photometric redshifts are poorly tested in the difficult spectroscopic redshift ranges of $1 \lesssim z \lesssim 2.5$ and $z \gtrsim 4$, as well as at the extremely faint flux limits plotted in Fig. 11. Finally, these surface densities are based on optically-selected objects. If a large population of dust-enshrouded galaxies exists, they may be missed in the optical surveys.

7.2. Star Formation Rates and the Cosmic Star Formation History

If the ionization is dominated by hot, young stars, the observed flux of the Lyα emission line may be used to estimate a lower bound to the star formation rate $\dot{M}$ in a galaxy. Using the case B recombination Lyα/Hα ratio of ≈ 10 (Osterbrock 1989), and the Kennicutt (1983) conversion from Hα luminosity to $\dot{M}$, Madau et al. (1998) find $\dot{M} \sim 0.7 \times 10^{-42}\ h_{50}^{-2}\ L_{{\rm Ly}\alpha}\ M_\odot\ {\rm yr}^{-1}$ where $L_{{\rm Ly}\alpha}$ is measured in units of ergs s^{-1} ($q_0 = 0.5$; $\dot{M}$ is ≈ 3.3 times larger for $q_0 = 0.1$). The star formation rate may also be estimated from the observed ultraviolet continuum emission. Madau et al. (1998) calculate that a population older than 100 Myr will have $\dot{M} \approx 10^{-40}\ L_{1500}\ M_\odot\ {\rm yr}^{-1}$ where L_{1500}, the luminosity at 1500 Å, is measured in units of ergs s^{-1}Å^{-1}. Leitherer, Carmelle, &

Heckman (1995) models yield similar results for a different IMF and ages less than 10 Myr. These are lower limits to $\dot{M}$ since no correction to the ultraviolet flux for either internal absorption or dust extinction has been made (see §7.5).

With sufficient numbers of well-observed distant systems, we may begin studying the star formation history of the Universe as a function of co-moving volume. The Canada-France Redshift Survey (CFRS; Lilly et al. 1995) demonstrated strong luminosity evolution in the blue field galaxy population between $z = 0$ and $z = 1$. Madau et al. (1996), using the early results of photometric selection in the HDF, integrated the results at $z < 5$ into a coherent picture of the star formation history of the Universe and suggested that the global star formation peaks between $z = 1$ and $z = 2$, in remarkable agreement with predictions based on the co-moving H I density traced by Lyα absorption systems (Pei & Fall 1995), with hierarchical models in a cold dark matter-dominated Universe (Baugh et al. 1998), and with the quasar luminosity function (Cavaliere & Vittorini 1998).

Substantial caveats temper this result, however: (1) the number of spectroscopically measured redshifts between $z = 1$ and $z = 2$ is small. Connolly et al. (1997) use optical and near-infrared data to estimate photometric redshifts in the HDF at $1 < z < 2$ in order to span this redshift "desert" for which few strong spectroscopic features are shifted into the optical regime. Until a substantial number of confirmed redshifts have been obtained, however, photometric redshifts in the $1 < z < 2$ range are not well constrained. Thus the epoch thought to be the most productive in terms of star formation is also the least well measured. (2) The small area ($\approx$ five square arcminutes) covered by the HDF makes global parameters inferred from it vulnerable to perturbations from large scale structure. (3) The existence of the peak at $z \sim 1.5$ is contingent upon the completeness of the estimates of global star formation at higher redshift. The $z \sim 4$ point in the analysis of Madau et al. (1996) was based on a single object in the HDF at $z = 4.02$ (Dickinson 1998) and should thus be treated as an uncertain lower limit. More recent measurements, based on larger-area surveys, show that the star formation density is significantly higher at $z \gtrsim 4$ (Steidel et al. 1999). Finally, (4) both the photometric and the Lyα search techniques require the objects to be UV-bright. It is possible that a substantial fraction of star-forming activity in dusty high-redshift systems has been overlooked thus far. The recent discoveries of a relatively large number of resolved sources in small area sub-mm surveys performed by SCUBA suggest this to be the case (e.g., Hughes et al. 1998; Barger et al. 1998; Dey et al. 1999).

Fig. 12 illustrates a recent determination of the star formation history of the Universe. In sharp contrast to the initial results of Madau et al. (1996), the UV luminosity density of the Universe is approximately constant at $2 \lesssim z \gtrsim 4$. Preliminary results from the Berkeley longslit searches suggest that it remains constant to $z \simeq 5.5$. The evolution of the star formation density of the Universe, as probed by apparently normal, star-forming systems, implies that their evolution follows a significantly different trajectory than that of AGN, especially quasars. Both radio-quiet and radio-loud quasars show a considerable density decrease beyond $z \sim 3$ (c.f., Dunlop & Peacock 1990; Hook & McMahon 1998; Cavaliere & Vittorini 1998), falling by a factor of ~ 3 from $z = 3$ to $z = 4$.

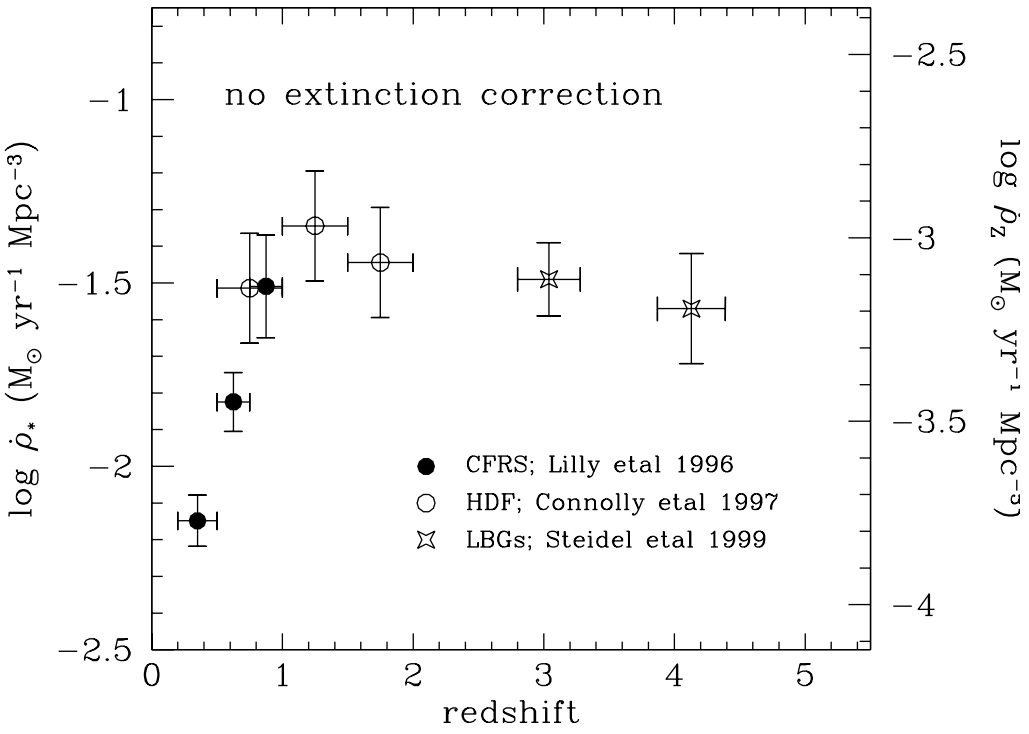

Fig. 12.— The star formation history of the Universe. Points at $z < 1$ are from the Canada France Redshift Survey (CFRS; Lilly et al. 1996); points at $1 \lesssim z \lesssim 2$ are from near-infrared studies of the HDF (Connolly et al. 1997); and points at $z \simeq 3$ and $z \simeq 4$ are from studies of Lyman-break galaxies (LBGs; Steidel et al. 1999). For a Salpeter IMF, the cosmic metal ejection density, $\dot{\rho}_z$, is 1/42 of the cosmic star formation density, $\dot{\rho}_*$ (Madau et al. 1996).

7.3. Effects of the IGM: Hints of the Gunn-Peterson Effect?

The ability of astronomers to calculate reliable photometric redshifts at $z > 3$ is largely due to the neutral hydrogen absorption in the intergalactic medium (IGM). Absorption below the redshifted Lyman limit, Lyβ, and Lyα strongly modulates the observed optical spectra of the objects we are interested in. At sufficiently high redshifts, the continuum depression blue-ward of Lyα (the Lyα forest) dominates over those decrements associated with higher members of the Lyman series. Oke & Koryanski (1982) define the D_A parameter to measure the strength of the Lyα decrement

$$D_A \equiv 1 - \frac{f_\nu(\lambda\lambda 1050 - 1170)_{\rm obs}}{f_\nu(\lambda\lambda 1050 - 1170)_{\rm pred}} \tag{3}$$

(see Fig. 13). The question is: at what redshift does the Lyα forest become an impenetrable "jungle"?

This is an intriguing question, as we are now observing galaxies at early-enough cosmic epoch that we may perhaps encounter the edge of the "Dark Era" — prior to the complete reionization

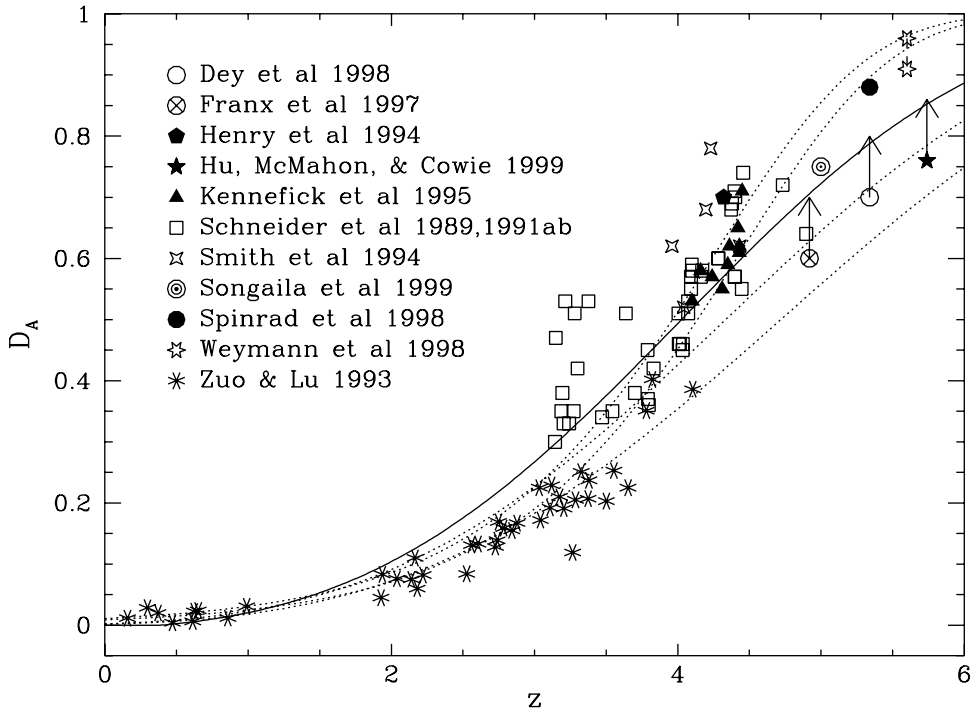

Fig. 13.— Values of the continuum depression blue-ward of Lyα (D_A; Oke & Koryanski 1982) plotted as a function of redshift from several observational samples (Dey et al. 1998; Franx et al. 1997; Henry et al. 1994; Hu et al. 1999; Kennefick et al. 1995; Schneider, Schmidt, & Gunn 1989; Schneider, Schmidt, & Gunn 1991a, 1991b; Smith et al. 1994; Songaila et al. 1999; Spinrad et al. 1998; Weymann et al. 1998; Zuo & Lu 1993). The Madau (1995) model (solid line) and several parametrizations from Zhang et al. (1997) (dotted lines) are also plotted (see text). Zuo & Lu (1993) may be systematically offset from the other measurements. At $z \gtrsim 5$ are we perhaps seeing the hints of hydrogen absorption in excess of what is expected from the Lyα forest alone? Could this be the first indications of the long-anticipated Gunn-Peterson effect?

of the IGM when the Universe is still optically thick below the rest wavelength of Lyα. Theoretical estimates suggest that the dark era ends between $z = 5$ and $z = 20$ (Shapiro 1995; Rees 1995; Miralda-Escude & Rees 1997; Madau et al. 1998). Observationally, we would expect a (Gunn-Peterson) trough of complete absorption for some interval short-ward of Lyα, corresponding to the epoch when the Universe was completely opaque to Lyα photons.

How can we measure the Gunn-Peterson effect? For objects of $I \sim 26$, the obvious problem is one of signal-to-noise ratio. Combining the results of our spectrophotometry with deep *HST* images, we measure rather large values of D_A for HDF 3-951.0 ($z = 5.34$; $D_A = 0.88$; Dey et al. 1998) and HDF 4-473.0 ($z = 5.60$; $D_A = 0.91 - 0.96$; Weymann et al. 1998). Our concern about the break amplitude arises from its strength: the Madau (1995) theoretical estimate of the contribution

of the Lyα forest to D_A (solid line in Fig. 13) is only ≈ 0.79 at $z = 5.34$ and ≈ 0.83 at $z = 5.60$. This extrapolation assumes a distribution of high and low optical depth foreground Lyα clouds causing Lyman series absorption in the spectrum of a distant quasar or galaxy. The dotted lines in Fig. 13 represent different models of D_A from Zhang et al. (1997). Using the data of Steidel & Sargent (1987) and Zuo & Lu (1993), they estimate the mean intergalactic Lyα opacity τ_α as a function of redshift using two parametrizations of τ_α: $\tau_\alpha = A(1+z)^{3.46}$ and $\tau_\alpha = Ae^{\beta(1+z)}$. The scatter around the theoretical curves is substantial, even at lower redshifts, so the high values of D_A at $z > 5$ may simply reflect the usual scatter observed in that parameter. However, the possibility to directly measure the epoch of reionization is not to be overlooked. The best chance for this will be with the discovery of a bright(er) object at $z > 5$, either in the form of a quasar, or a magnified galaxy behind a rich galaxy cluster.

7.4. Morphology

At $z = 5$, the Universe is only 890 h_{50}^{-1} Myr old, corresponding to a lookback time of 93.2% of the age of the Universe. Any galaxies observed at these early epochs must necessarily be in their youth, and any information we can obtain on them is of the utmost interest to studies of galaxy formation. In particular, if these galaxies are truly primeval objects forming their first generation of stars, their morphologies can provide constraints on galaxy formation models. If the formation of a galactic spheroid occurs via the monolithic collapse of a protogalactic cloud (e.g., Eggen et al. 1962), then the bulk of its star formation might occur in a small region kiloparsecs in extent; such high-redshift protogalaxies will appear as compact, luminous objects (Lin & Murray 1992). Alternatively, if galaxy formation is a hierarchical process (e.g., Baron & White 1987; Baugh et al. 1998), protogalaxies may appear as a multitude of unresolved subgalactic clumps embedded in a more diffuse gaseous halo.

All of the confirmed $z > 4$ galaxies in the HDF (Fig. 14) have compact, but resolved morphologies, with deconvolved half-light radii of $\approx 0\farcs2$ ($\approx 1 - 2\ h_{50}^{-1}$ kpc), comparable to the values found for many of the $z \sim 3$ Lyman-break galaxies (Giavalisco et al. 1996). The sizes are clearly sub-galactic, suggestive of the hierarchical scenarios of galaxy formation. HDF 3-951.1, the brighter component of HDF 3-951.0 ($z = 5.33$ for both), contains substructure with a second "hot spot" approximately $0\farcs12$ east of the core, at a projected separation of 0.66 h_{50}^{-1} kpc. We speculate that this is either a knot of star formation (bright in the rest-frame ultraviolet), or evidence of multiple nuclei. The projected proximity of HDF 3-951.2 adds weight to the hypothesis that this is a dynamically-bound system, and that we are witnessing a merger event. HDF 4-439.0 at $z = 4.54$ and HDF 4-625.0 at $z = 4.58$ also both have multiple components. Lyman-break galaxies at $z \sim 3$ often exhibit either disrupted morphologies or multiple components (e.g., Giavalisco et al. 1996; Steidel et al. 1996b; Bunker, Moustakas, & Davis 1999). However, HDF 4-473.0 at $z = 5.60$ shows no evidence of substructure.

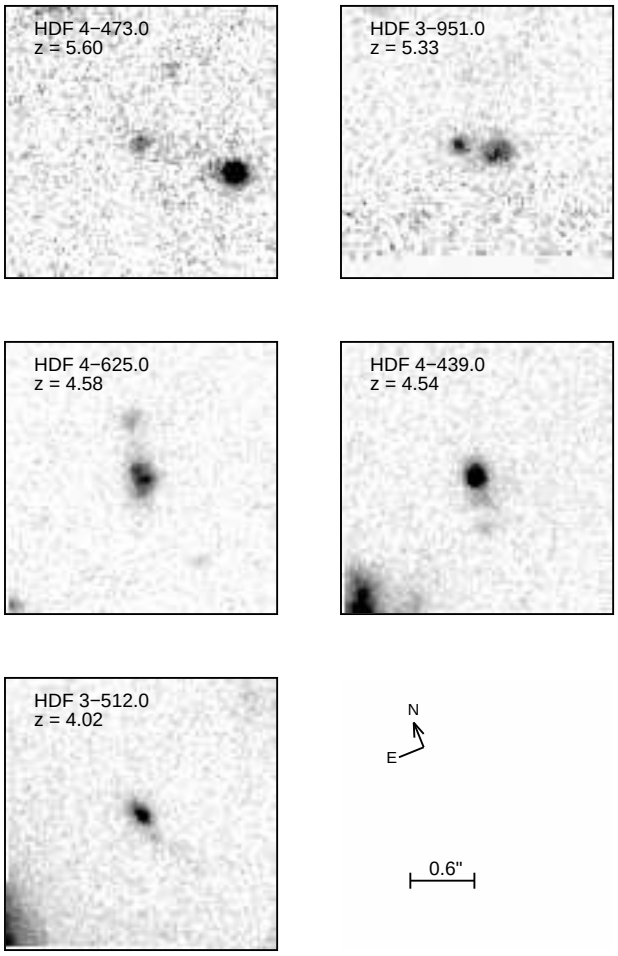

Fig. 14.— Montage of spectroscopically-confirmed $z > 4$ galaxies in the HDF, from the drizzled F814W (I_{814}) images. Note that most of the galaxies are compact, but show evidence of merging activity (interactions), in the form of multiple nuclei, multiple components, and/or extended, low-surface brightness tidal tails.

7.5. The Role of Dust

Since most of our observations sample restframe ultraviolet wavelengths, derived quantities such as star formation rates are sensitive to gas and dust extinction. As noted earlier, Lyα is particularly vulnerable since it is a resonance line whose escape is dependent upon the distribution of neutral gas.

One method of estimating the amount of reddening, used by Meurer et al. (1997); Pettini et al. (1999a); Dickinson (1998); Bunker et al. (1999); Steidel et al. (1999), is to assume a very young ($\approx 10^7$ yr age) starburst and ascribe any color excess in the emitted ultraviolet to extinction. The uncertainty, of course, is that aging of a starburst will also cause reddening. Typical extinction corrections are factors of $2-7$ near 1500 Å, depending upon the extinction law applied. Meurer et al. (1997) derive a correction factor of ≈ 15, in part due to different assumptions regarding the spectral slope of the underlying, unreddened population.

Near-infrared photometry offers the possibility of more reliable estimates of reddening, since at these wavelengths photometry is insensitive to the details and ages of the hottest stars. The ground-based (Keck/NIRC) J-band detection of 0140+326 RD1 by Armus et al. (1998) suggests substantial reddening ($A_V > 0.5$, for Bruzual & Charlot (1993) models with ages less than 10^8 yr), which is somewhat surprising given its non-detection in deep sub-mm observations, strong Lyα emission, and similar star formation rates inferred from its rest-frame ultraviolet continuum and Lyα flux density.

HST/NICMOS imaging offers deep, reliable near-infrared photometry and will be a valuable asset for measuring reddening in Lyman-break galaxies. For example, Weymann et al. (1998) use NICMOS F110W and F160W photometry to limit the reddening and star formation rate of HDF 4-473.0 ($z = 5.60$). They find that the spectral energy distribution limits the reddening to $0.00 \lesssim E(B-V) \lesssim 0.12$ and the star formation rate to $8\ M_\odot\ \mathrm{yr}^{-1} \lesssim \dot{M} \lesssim 19\ M_\odot\ \mathrm{yr}^{-1}$. This modest amount of extinction is consistent with the rather strong Lyα emission line emerging from this distant galaxy.

Near-infrared spectroscopy offers a potent tool for studying the dust content, mass, age, and kinematics of distant galaxies. Pettini et al. (1998) recently reported a pilot program of near-infrared spectra of the well-studied, rest-frame optical, nebular emission lines from H II regions in five Lyman-break galaxies at $z \simeq 3$. The observations used the CGS4 spectrometer on the United Kingdom Infrared Telescope and targeted the redshifted Balmer and [O III] emission lines. Hβ luminosities, uncorrected for intrinsic dust extinction, imply star formation rates of $20-270\ h_{70}^{-2}\ M_\odot\ \mathrm{yr}^{-1}$ ($q_0 = 0.1$); that is, typically a factor of several larger than that inferred from the UV continuum of these galaxies. The implication is that an extinction of $1-2$ magnitudes at 1500 Å may be typical of the Lyman-break population. Velocity dispersions of $\sigma \simeq 70\ \mathrm{km\,s^{-1}}$were reported in four out of the five galaxies, suggesting virial masses $M_{\mathrm{vir}} \approx (1-5) \times 10^{10}\ M_\odot$. The relative redshifts of Lyα emission, interstellar absorption, and nebular emission lines vary by several hundred $\mathrm{km\,s^{-1}}$, suggestive of large-scale outflows. Similar scale outflows are common in regions of rapid star formation locally.

Future higher-resolution (spectral and spatial) observations of these and related rest-frame optical transitions redshifted into the near-infrared should better address the kinematics and possibly the light-element abundances of young, forming galaxies.

7.6. Galaxy Clustering at High Redshift

Astronomers generally assume that the galaxy distribution traces the underlying matter distribution; comparisons of the large-scale distribution of galaxies at early cosmic epoch therefore is a potentially powerful means of discriminating cosmology and mechanisms of structure formation (e.g., White 1997). A simple constant of proportionality known as the "bias parameter", b, relating galaxy and mass fluctuations, is the conventional parametrization: $\delta_{\rm gal} = b\delta_{\rm mass}$. In principle, many physical mechanisms could lead to a relation of this form (e.g., Dekel & Rees 1987), though gravitational instability in a massive dark matter halo is currently popular as numerical simulations and semi-analytic models of this "dark halo" model are consistent with observations (e.g., Baugh et al. 1998; Mo, Mao, & White 1999).

Sufficient numbers of galaxies at $z \gtrsim 3$ have now been reliably identified that observational measurements of their spatial distribution is now possible. Giavalisco et al. (1998) reports on the angular clustering of Lyman-break galaxies at $z \sim 3$. The slope of a power-law parametrization of the angular correlation function, $w(\theta) = A_w\theta^{-\beta}$, is $\beta \sim 0.9$, similar to galaxy samples in the local and intermediate-redshift Universe. Applying the Limber transform to $w(\theta)$ yields the comoving spatial correlation length. Giavalisco et al. (1998) report $r_0 = 4.2^{+0.9}_{-1.0}\ h_{50}^{-1}$ Mpc ($q_0 = 0.5$) at the median redshift of their Lyman-break survey, $\bar{z} = 3.04$. The value is similar to that of local spiral galaxies and approximately half that of local early-type galaxies; it is comparable or slightly larger than comoving spatial correlation lengths determined for intermediate-redshift galaxies. The strong clustering is broadly consistent with biased galaxy formation theories, suggesting that the Lyman-break systems are associated with massive dark matter halos.

Steidel et al. (1998) report a large structure of Lyman-break galaxies at $z \simeq 3.09$ in the SSA22 field which they interpret in the context of cold dark matter cosmological models. Dark halo models of galaxy formation predict that galaxies of a given mass should form first in regions of the highest density and that these regions should be strongly clustered spatially. Adelberger et al. (1998) measure the bias parameter, b for the Steidel et al. (1998) $z \simeq 3.09$ structure: considering 268 Lyman-break galaxies in six $9' \times 9'$ fields with spectroscopic redshifts at $z \simeq 3$, Adelberger et al. (1998) perform a counts-in-cell analysis, measuring the fluctuations in galaxy counts in cells of differing comoving volume. They find that the variance in cubes of comoving side length $(15.4, 23.8, 22.8)\ h_{50}^{-1}$ Mpc is $\sigma^2_{\rm gal} \sim 1.3 \pm 0.4$. Following the methodology of Peacock & Dodds (1994), the implied bias factor is $b = (6.0 \pm 1.1, 1.9 \pm 0.4, 4.0 \pm 0.7)$ for these spatial scales. The result is broadly consistent with simple dark halo models of structure formation, in which matter fluctuations are Gaussian, have a linear power-spectrum shape similar to that determined locally ($\Gamma \sim 0.2$), and Lyman-break galaxy luminosities are correlated with their mass. The results are largely independent of cosmology. Adelberger et al. (1998) note that measurements of the Lyman-break galaxy masses could, in principal, distinguish cosmological scenarios.

7.7. A Brief Comparison to Theories of Galaxy Formation

The Pritchet (1994) review on primeval galaxies speculates that progenitors of galaxies like our Milky Way should be very numerous, regardless of appearance. The data, in the form of images and spectra of distant $z \gtrsim 3$ Lyman-break systems and faint number counts, currently suggests that galaxies start as many smaller subclumps and halos so that the local density of L^* galaxies ($0.015\ h_{50}^3$ Mpc^{-3}) may substantially underestimate the co-moving space density of small objects at $z = 5$.

The dominant paradigm for understanding the Lyman-break population is the "dark halo" model: galaxies quiescently form stars at the bottom of the potential wells of massive dark matter halos. Assuming rest-frame UV luminosities correlate with galaxy mass, the brightest Lyman-break galaxies should form first in regions where the density is highest. Since these regions are expected to be strongly clustered spatially, the high-redshift, large-scale structures discussed in §7.6 are explained naturally. Over time, the halos merge, forming the massive galaxies we see locally.

Baugh et al. (1998) present a semianalytic model of this hierarchical galaxy formation scenario, focusing on the properties of Lyman-break galaxies at $z \simeq 3$. With a "suitable" choice of parameters, they are able to reproduce the observed Lyman-break galaxy properties for cold dark matter (CDM) cosmologies with both $\Omega_0 = 1$ and $\Omega_0 < 1$. At high redshift, galaxies have very small bulges or no bulge at all: typical half-light radii are $\sim 1\ h_{50}^{-1}$ kpc, in good agreement with the $z \sim 3$ results of Giavalisco et al. (1996) and the HDF images at $z > 4$. Baugh et al. (1998) also reproduce the strongly biased spatial distribution, with $b \simeq 4$ and a comoving correlation length $r_0 \simeq 8\ h_{50}^{-1}$ Mpc at $z \simeq 3$. These models predict that the average L^* galaxy today was in ≈ 4 sub-units at $z = 1$ and ≈ 14 sub-units at $z = 5$.

However, the Baugh et al. (1998) models fair less well with respect to star formation rates. They predict that at $z \simeq 3$, most galaxies are only forming a few solar masses of stars per year and only a very small fraction have star formation rates in excess of $40\ h_{50}^{-2}\ M_\odot\ \mathrm{yr}^{-1}$. This is at odds with more recent estimates of the rest-UV extinction of the $z \simeq 3$ Lyman-break population, e.g., the near-infrared spectroscopic results of Pettini et al. (1998). The hierarchical models also predict that galaxies form the bulk of their stars at relatively low redshift (e.g., Baron & White 1987), with $\simeq 50\%$ of the stars formed since $z \simeq 1$. The Baugh et al. (1998) models predict that cosmic star formation history peaks around $z = 1 - 2$, in rough concordance with the first measurements of the comoving star formation history by Madau et al. (1996). More recent measurements, discussed in §7.2, still show the rapid evolution in comoving star formation rate from $z = 0$ to $z \sim 1.5$, but, with larger samples of high-redshift objects less vulnerable to cosmic variance and improved consideration of rest-frame UV extinction, the revised plots show a plateau in the comoving star formation density from $z \sim 1.5$ to $z \sim 4$ (Fig. 12).

An alternate view of the Lyman-break population maintains that these galaxies are primarily collision-induced galactic starbursts, triggered by small, gas-rich satellite galaxies (Lowenthal et al. 1997; Somerville, Primack, & Faber 1999; Kolatt et al. 1999). Using semianalytic models,

Somerville et al. (1999) study the properties of individual galaxies in the "quiescent" dark halo scenario, similar to that addressed by Baugh et al. (1998), in comparison to the "collisional starburst" scenario. They argue that the high star-formation rates, small nebular emission line widths (~ 70 km s^{-1}; Pettini et al. 1998), young ages (median age ~ 25 Myr; Sawicki & Yee 1998), and high surface densities are all better explained by the collisional starburst model. More recently, Kolatt et al. (1999) use high-resolution N-body simulations to address the clustering properties of Lyman-break sources in the collisional starburst model. They find that although most sources are relatively low mass in this scenario, they cluster around high-mass halos and therefore exhibit the observed strongly biased clustering.

8. Conclusions and Thoughts for the New Millennium

Progress in the field of distant galaxies has been rapid. Young, star-forming galaxies have been located by several means, and studied from space and the ground to magnitudes as faint as $V = 28$ and redshifts as large as $z = 5.7$, perhaps to even $z = 6.7$ or higher. A population of faint, dusty galaxies has been detected in the sub-mm region; their redshift distribution remains uncertain for now.

Observations with *HST* have established the prevalence of small protogalaxy candidates at high redshift. How and when do they merge to form the familiar Hubble types observed locally?

The last review of the subject of primeval galaxies in this journal, only five years ago, was largely a census of non-detection limits and a discussion of theoretical expectations of the predicted wide-spread population of young galaxies at high redshift (Pritchet 1994). The field is expanding so fast now that this review will be largely outdated at the time of press. We conclude with a brief discussion of ripe avenues for the field of deep extragalactic studies. Several of the next steps will involve new instruments and satellites slated for commissioning in the coming months and years. We also suggest some ventures to longer wavelengths that those typically employed in contemporary early Universe studies. It is, of course, the redshift that pushes us in that direction.

- Currently, much of the early Universe extragalactic research has focussed on simply procuring redshifts, identifying objects at earlier and earlier cosmic epoch, and studying the spatial clustering of (the Lyman-break) population. Spectroscopy has the potential to provide considerably more information. Detailed, higher-resolution, higher signal-to-noise ratio observations of some of the brighter Lyman-break galaxies can probe the ages, kinematics, and abundances of young (proto-)galaxies. Spinrad et al. (1999) suggests, from a very limited sample, that Lyα emission strength anticorrelates with the strength of the rest-frame UV interstellar absorption lines. More recently, Pettini et al. (1999b) have reported on intermediate resolution, high signal-to-noise ratio spectroscopy of the lensed galaxy MS 1512−cB58 at $z = 2.727$. This detailed study probes the stellar initial mass function (IMF) at early cosmic epoch, finding no evidence for a flatter IMF (at the high-mass end) or an IMF deficient in high-mass stars.

They measure a metallicity of ≈ 0.25 solar and bulk outward motions of 200 $\mathrm{km\,s^{-1}}$, which may be an important mechanism of distributing metals in the IGM. This pioneering study lays the groundwork for follow-up studies on larger samples of (unlensed) sources.

- The new generation of near-infrared spectrographs on large-aperture, ground-based telescopes such as the Keck Near Infrared Spectrometer (NIRSPEC) and the Very Large Telescope (VLT) Infrared Spectrometer And Array Camera (ISAAC), opens the window on observing the early Universe to unprecedented redshifts. The first near-infrared detection of Lyα emission will be a technological feat. What search techniques will prove most efficient at identifying sources at $z \approx 10$, assuming that sufficiently luminous sources have collapsed at that redshift? These cameras should be sensitive to line emission at flux densities $\sim 10^{-17}\,\mathrm{ergs\,cm^{-2}\,s^{-1}}$ out to $\sim 2.5\mu$m in the windows between telluric OH emission. An hour spectrum with a 10 m telescope at resolving power $R \sim 2000$ should yield a detection at a signal-to-noise ratio $S/N \sim 5$ for an unresolved emission line of that strength. A more-realistic, slightly-resolved (spatially and spectrally) emission line would require several hours to yield a S/N of a few per resolution element. Detection of the anticipated 0.5μJy continuum longward of Lyα will remain challenging: NIRSPEC, as an example, will require $\approx$ six hours on integration to reach $S/N \sim 1$ per resolution element; multiple-binning will be requisite.

- Several new telescopes, cameras, and satellite missions are expected to be commissioned shortly. At sub-mm wavelengths, more-sensitive cameras with improved spatial resolution such as SCUBA+ and BOLOCAM will be having first light in the next few years. Satellites such as *SIRTF*, *Chandra*, and *XMM* will open up the mid-infrared and X-ray universe considerably.

- With the prospect of *NGST* becoming more realistic, one can consider deep imaging and spectroscopy in the infrared, perhaps to $\sim 4\mu$m. This would open up the "dark age" to extreme, unprecedented redshifts; at $z = 25$, Lyα propogates to 3.16μm and we are probing the Universe at a time less than 100 h_{50}^{-1} Myr after the Big Bang. Imaging above and below this wavelength might be an excellent diagnostic for the very early quasars, galaxies, and supernovae.

- The mm-region of the spectrum has been a good region for molecular studies of our Milky Way galaxy. In the future it may also be the domain of choice for redshift coolant lines such as [C II]$\lambda 158\mu$m. This transition is potentially strong in both H I and H II regions; some local starbursts emit between 10^{-2} and 10^{-3} of the infrared (dust) continuum in this line. Its application to large redshifts is still uncommon, but unless the C/H ratio in young galaxies is disastrously low, it seems worth attempting detection of high redshift [C II]$\lambda 158\mu$m with modern mm-interferometers. At $z = 7$, for example, the line redshifts to 1.26 mm. The opportunity then would be substantial – even for some physical study of a very distant (gas-rich) stellar system.

We are indebted to our close collaborators Andrew Bunker and Arjun Dey for extensive conversations on the subject of distant galaxies and helping shape our conception of the deep Universe. We also gratefully acknowledge conversations and communications with Kurt Adelberger, Len Cowie, Carlos De Breuck, Mark Dickinson, George Djorgovski, Peter Eisenhardt, James Graham, Esther Hu, Ken Lanzetta, Curtis Manning, Pat McCarthy, Ed Moran, Leonidas Moustakas, George Smoot, Adam Stanford, Chuck Steidel, Eduard Thommes, Wil van Breugel, and Rogier Windhorst. We thank Alberto Fernández-Soto for providing Fig. 7, Ken Lanzetta for providing Fig. 11, Trinh Thuan for sharing the *HST*/GHRS spectrum of T1214−277, and Dave Hollenbach for conversations regarding the [C II]λ158μm emission line strength. We are also indebted to Sam Maxie for considerable typographical efforts on the early draft of this manuscript. We acknowledge NSF Grant AST 95−28536 for supporting some of the extragalactic research presented herein. Research by DS has been supported by IGPP/LLNL grant 98−AP017.

REFERENCES

Adelberger, K. L., Steidel, C. C., Giavalisco, M., Dickinson, M., Pettini, M., & Kellogg, M. 1998, ApJ, 505, 18

Akerlof, C. et al. 1999, Nature, 398, 400

Armus, L., Matthews, K., Neugebauer, G., & Soifer, B. T. 1998, ApJ, 506, 89

Barger, A., Cowie, L., Sanders, D., Fulton, E., Taniguchi, Y., Sato, Y., Kaware, K., & Okuda, H. 1998, Nature, 394, 248

Barger, A., Cowie, L. L., Smail, I., Ivison, R. J., Blain, A. W., & Kneib, J.-P. 1999, AJ, 117, 2656

Baron, E. & White, S. 1987, ApJ, 322, 585

Barvainis, R., Tacconi, L., Antonucci, R., Alloin, D., & Coleman, P. 1994, Nature, 371, 586

Baugh, C. M., Cole, S., Frenk, C. S., & Lacey, C. G. 1998, ApJ, 498, 504

Baum, S. & Heckman, T. 1989, ApJ, 336, 702

Baum, W. A. 1962, in *Problems of Extragalactic Research*, ed. G. C. McVittie, Vol. 51 (New York: Macmilliam, IAU Symposia), 390

Becker, R. H., White, R. L., & Helfand, D. J. 1995, ApJ, 450, 559

Benítez, N. 1999, ApJ, submitted, astro-ph/9811189

Bennett, A. S. 1961, MmRAS, 68, 163

Bennett, C. L. et al. 1996, ApJ, 464, 1

Best, P. N., Longair, M. S., & Röttgering, H. J. A. 1996, MNRAS, 280, 9

Blain, A. & Longair, M. 1993, MNRAS, 264, 509

Bloom, J. S. et al. 1999, ApJ, 518, 1

Brunner, R. J., Connolly, A. J., Szalay, A. S., & Bershady, M. A. 1997, ApJ, 482, L21

Bruzual, A. G. & Charlot, S. 1993, ApJ, 405, 538

Bunker, A. J., Moustakas, L. A., & Davis, M. 1999, ApJ, in press

Calzetti, D., Kinney, A. L., & Storchi-Bergmann, T. 1994, ApJ, 429, 582

Carilli, C. L., Harris, D. E., Pentericci, L., Roettgering, H. J. A., Miley, G. K., & Bremer, M. N. 1998, ApJ, 494, 143

Carilli, C. L. & Yun, M. S. 1999, ApJ, 513, 13

Cavaliere, A. & Vittorini, V. 1998, in *The Young Universe: Galaxy Formation and Evolution at Intermeidiate and High Redshift*, ed. S. D.'Odorico, A. Fontana, & E. Giallongo, Vol. 146 (San Francisco: ASP Conference Series), 26

Chambers, K. C., Miley, G. K., & van Breugel, W. J. M. 1987, Nature, 329, 604

—. 1990, ApJ, 363, 21

Charlot, S. & Fall, S. M. 1993, ApJ, 378, 471

Chen, H.-W., Lanzetta, K. M., & Pascarelle, S. 1999, Nature, 398, 586

Cheng, Y.-C. & Krauss, L. M. 1999, New Astronomy, submitted, astro-ph/9908292

Cimatti, A., Dey, A., van Breugel, W., Antonucci, R., & Spinrad, H. 1996, ApJ, 465, 145

Cimatti, A., Dey, A., van Breugel, W., Hurt, T., & Antonucci, R. 1997, ApJ, 476, 677

Coleman, G. D., Wu, C.-C., & Weedman, D. W. 1980, ApJS, 43, 393

Connolly, A. J., Csabai, I., Szalay, A. S., Koo, D. C., Kron, R. C., & Munn, J. A. 1995, AJ, 110, 2655

Connolly, A. J., Szalay, A. S., Dickinson, M., Subbarao, M. U., & Brunner, R. J. 1997, ApJ, 486, 11

Cowie, L. & Hu, E. M. 1998, AJ, 115, 1319

Crampton, D. 2000, in *Photometric Redshifts and High-Redshift Galaxies*, ed. R. Weymann, L. Storrie-Lombardi, M. Sawicki, & R. Brunner (San Francisco: ASP Conference Series), in press

De Breuck, C. et al. 1999, AJ, submitted

Dekel, A. & Rees, M. J. 1987, Nature, 326, 455

Deltorn, J.-M., Le Fevre, O., Crampton, D., & Dickinson, M. 1997, ApJ, 483, L21

Dey, A. 1999, in *The Most Disant Radio Galaxies*, ed. H. Röttgering, P. N. Best, & M. D. Lehnert (Dordrecht: Kluwer), 19

Dey, A., Cimatti, A., van Breugel, W., Antonucci, R., & Spinrad, H. 1996, ApJ, 465, 157

Dey, A., Graham, J. R., Ivison, R. J., Smail, I., Wright, G. S., & Liu, M. C. 1999, ApJ, 519, 610

Dey, A., Spinrad, H., Stern, D., Graham, J. R., & Chaffee, F. 1998, ApJ, 498, L93

Dey, A., van Breugel, W., Vacca, W. D., & Antonucci, R. 1997, ApJ, 490, 698

Dey, A. et al. 2000, ApJ, in preparation

Dickinson, M. 1995, in *Fresh Views of Elliptical Galaxies*, ed. A. Buzzoni, A. Renzini, & A. Serrano, Vol. 86 (San Francisco: ASP Conference Series), 283

Dickinson, M. 1998, in *The Hubble Deep Field*, ed. M. Livio, M. Fall, & P. Madau, Vol. 11 (New York: Cambridge Univ. Press, STScI Symposia), 219

Dickson, R., Tadhunter, C., Shaw, M., Clark, N., & Morganti, R. 1995, MNRAS, 273, 29

Djorgovski, S. G. 1995, in *Science with the VLT*, ed. J. R. Walsh & I. J. Danziger (Berlin: Springer Verlag), 351

Djorgovski, S. G., Odewahn, S. C., Gal, R. R., Brunner, R., & de Calvalho, R. R. 2000, in *The Hy-Redshift Universe*, ed. A. J. Bunker & W. van Breugel (San Francisco: ASP Conference Series), in press

Djorgovski, S. G., Pahre, M. A., Bechtold, J., & Elston, R. 1996, Nature, 382, 234

Djorgovski, S. G., Spinrad, H., McCarthy, P., Dickinson, M., van Breugel, W., & Strom, R. G. 1988, AJ, 96, 836

Djorgovski, S. G., Spinrad, H., McCarthy, P., & Strauss, M. A. 1985, ApJ, 299, L1

Dunlop, J. S. & Peacock, J. A. 1990, MNRAS, 247, 19

—. 1993, MNRAS, 263, 936

Dunlop, J. S., Peacock, J. A., Spinrad, H., Dey, A., Jimenez, R., Stern, D., & Windhorst, R. A. 1996, Nature, 381, 581

Eales, S. & Rawlings, S. 1993, ApJ, 411, 67

—. 1996, ApJ, 460, 68

Eggen, O. C., Lynden-Bell, D., & Sandage, A. R. 1962, ApJ, 136, 748

Eisenhardt, P. R., Armus, L., Hogg, D., Soifer, B. T., Neugebauer, G., & Werner, M. W. 1996, ApJ, 461, 72

Eke, V. R., Cole, S., & Frenk, C. S. 1996, MNRAS, 282, 263

Elston, R., McCarthy, P. J., Eisenhardt, P., n, M. D., & Spinrad, H. 1994, AJ, 107, 910

Fabbiano, G. 1989, ARA&A, 27, 87

Fabian, A. C., Brandt, W. N., McMahon, R. G., & Hook, I. M. 1997, MNRAS, 291, 5p

Fan, X. et al. 1999, AJ, 118, 1

Fernàndez-Soto, A., Lanzetta, K., & Yahil, A. 1999, ApJ, 513, 34

Francis, P. J. et al. 1996, ApJ, 457, 490

Franx, M., Illingworth, G. D., Kelson, D. D., van Dokkum, P. G., & Tran, K.-V. 1997, ApJ, 486, L75

Frye, B. & Broadhurst, T. J. 1998, ApJ, 499, 115

Georgantopoulos, G. et al. 1996, MNRAS, 280, 276

Giavalisco, M., Steidel, C. C., Adelberger, K. L., Dickinson, M. E., Pettini, M., & Kellogg, M. 1998, ApJ, 503, 543

Giavalisco, M., Steidel, C. C., & Macchetto, D. 1996, ApJ, 470, 189

Goodman, J. 1986, ApJ, 308, L17

Graham, J. R. & Liu, M. C. 1995, ApJ, 449, L29

Guzmàn, R. et al. 1997, ApJ, 489, 559

Gwyn, S. D. J. 2000, in *Photometric Redshifts and High-Redshift Galaxies*, ed. R. Weymann, L. Storrie-Lombardi, M. Sawicki, & R. Brunner (San Francisco: ASP Conference Series), in press

Gwyn, S. D. J. & Hartwick, F. D. A. 1996, ApJ, 468, L77

Hales, S. E. G., Baldwin, J. E., & Warner, P. J. 1993, MNRAS, 234, 919

Hamann, F. & Ferland, G. 1999, ARA&A, in press, astro-ph/9904223

Hammer, F. et al. 1997, ApJ, 481, 49

Hartmann, L. W., Huchra, J. P., & Geller, M. J. 1984, ApJ, 287, 487

Hartmann, L. W., Huchra, J. P., Geller, M. J., O'Brien, P., & Wilson, R. 1988, ApJ, 326, 101

Hasinger, G., Burg, R., Giacconi, R., Schmidt, M., Trümper, J., & Zamorani, G. 1998, A&A, 329, 482

Henry, J. et al. 1994, AJ, 107, 1270

Hogg, D. W. et al. 1998, ApJ, 504, 622

Holland, W. S. et al. 1999, MNRAS, 303, 659

Hook, I. M. & McMahon, R. G. 1998, MNRAS, 294, L7

Hu, E. M., Cowie, L. L., & McMahon, R. G. 1998, ApJ, 502, 99

Hu, E. M. & McMahon, R. G. 1996, Nature, 382, 231

Hu, E. M., McMahon, R. G., & Cowie, L. L. 1999, ApJ, 522, 9

Hu, E. M., McMahon, R. G., & Egami, E. 1996, ApJ, 459, L53

Hughes, D. et al. 1998, Nature, 394, 241

Humason, M. L., Mayall, N. U., & Sandage, A. R. 1956, AJ, 61, 97

Jannuzi, B. T., Elston, R., Schmidt, G., Smith, P., & Stockman, H. 1995, ApJ, 454, L111

Kauffmann, G. & Charlot, S. 1998, MNRAS, 294, 705

Keel, K. I. & Windhorst, R. A. 1991, ApJ, 383, 135

Kelson, D. D., Illingworth, G. D., Franx, M., Magee, D., & van Dokkum, P. G. 1999, IAU Circ., 7096

Kennefick, J. D., Djorgovski, S. G., & de Calvalho, R. R. 1995, AJ, 110, 2553

Kennicutt, R. 1983, ApJ, 282, 54

—. 1992, ApJ, 388, 310

Kinney, A. L., Bohlin, R. C., Calzetti, D., Panagia, N., & Wyse, R. F. G. 1993, ApJS, 86, 5

Kolatt, T. S., Bullock, J. S., Somerville, R. S., Sigad, Y., aand A. V. Kravtsov, P. J., Klypin, A. A., Primack, J. R., Faber, S. M., et al. 1999, ApJ, 523, 109

Koo, D. C. 1985, AJ, 90, 418

Kulkarni, S. R. et al. 1998, Nature, 393, 35

Kunth, D., Lequeux, J., Sargent, W. L. W., & Viallefond, F. 1994, A&A, 282, 709

Kunth, D., Mas-Hesse, J. M., Terlevich, E., Terlevich, R., & Fall, S. M. 1998, A&A, 334, 11

Kunth, D., Terlevich, E., Terlevich, R., & Tenorio-Tagle, G. 1999, in *Dwarf Galaxies and Cosmology*, ed. T. X. Thuan (Gif-sur-Yvette: Editions Frontieres), in press

Lacy, M. et al. 1994, MNRAS, 271, 504L

Lanzetta, K. 2000, in *The Hy-Redshift Universe*, ed. A. J. Bunker & W. van Breugel (San Francisco: ASP Conference Series), in press

Lanzetta, K., Yahil, A., & Fernàndez-Soto, A. 1996, Nature, 381, 759

Leitherer, C., Carmelle, R., & Heckman, T. M. 1995, ApJS, 99, 173

Lilly, S. J. 1988, ApJ, 333, L161

Lilly, S. J., Eales, S. A., Gear, W. K., Hammer, F., Le Févre, O., Crampton, D., Bond, J. R., & Dunne, L. 1999, ApJ, 518, 641

Lilly, S. J., Fevre, O. L., Hammer, F., & Crampton, D. 1996, ApJ, 460, L1

Lilly, S. J. & Longair, M. S. 1982, MNRAS, 199, 1053

—. 1984, MNRAS, 211, 833

Lilly, S. J., Tresse, L., Hammer, F., Crampton, D., & Fevre, O. L. 1995, ApJ, 455, 108

Lin, D. N. C. & Murray, S. D. 1992, ApJ, 394, 523

Loeb, A. 1993, ApJ, 403, 542

Lowenthal, J. D. et al. 1997, ApJ, 481, 673

Lu, L., Sargent, W. L. W., Barlow, T. A., Churchill, C. W., & Vogt, S. S. 1996, ApJS, 107, 475

Madau, P. 1995, ApJ, 441, 18

Madau, P., Ferguson, H. C., Dickinson, M. E., Giavalisco, M., Steidel, C. C., & Fruchter, A. 1996, MNRAS, 283, 1388

Madau, P., Pozzetti, L., & Dickinson, M. E. 1998, ApJ, 498, 106

Malkan, M., Teplitz, H. I., & McLean, I. S. 1995, ApJ, 448, 5

Manning, C., Stern, D., Spinrad, H., & Bunker, A. J. 2000, ApJ, in preparation

Matthews, T. A., Morgan, W. W., & Schmidt, M. 1964, ApJ, 140, 35

McCarthy, P. J. 1993, ARA&A, 31, 639

McCarthy, P. J. 1999, in *The Most Disant Radio Galaxies*, ed. H. Röttgering, P. N. Best, & M. D. Lehnert (Dordrecht: Kluwer)

McCarthy, P. J., Baum, S. A., & Spinrad, H. 1996, ApJS, 106, 281

McCarthy, P. J., Spinrad, H., & van Breugel, W. 1995, ApJS, 99, 27

McCarthy, P. J., van Breugel, W., Spinrad, H., & Djorgovski, S. 1987, ApJ, 321, 29

McCarthy, P. J. et al. 1999, ApJ, 520, 548

Meurer, G. R., Heckman, T. M., Lehnert, M. D., Leitherer, C., & Lowenthal, J. 1997, AJ, 114, 54

Minkowski, R. 1960, ApJ, 132, 908

Miralda-Escude, J. & Rees, M. 1997, ApJ, 478, L57

Mo, H., Mao, S., & White, S. 1999, MNRAS, 304, 175

Mobasher, B., Rowan-Robinson, M., Georgakakis, A., & Eaton, N. 1996, MNRAS, 282, L7

Neuschaefer, L. W. & Windhorst, R. A. 1995, ApJS, 96, 371

Oke, J. B. & Koryanski, D. 1982, ApJ, 255, 11

Oke, J. B. et al. 1995, PASP, 107, 375

Osterbrock, D. 1989, *The Astrophysics of Gaseous Nebulae and Active Galactic Nuclei* (Mill Valley: Univ. Science Books)

Paczynski, B. 1986, ApJ, 308, L13

—. 1998, ApJ, 494, L45

Pascarelle, S. M., Windhorst, R. A., Keel, W. C., & Odewahn, S. C. 1996, Nature, 383, 45

Peacock, J. A. & Dodds, S. J. 1994, MNRAS, 267, 1020

Pei, C. & Fall, S. M. 1995, ApJ, 454, 69

Pentericci, L., Roettgering, H. J. A., Miley, G. K., Carilli, C. L., & McCarthy, P. 1997, A&A, 326, 580

Petitjean, P., Pecontal, E., Vals-Gebaud, D., & Charlot, S. 1996, Nature, 380, 411

Pettini, M., Ellison, S. L., Steidel, C. C., & Bowen, D. V. 1999a, ApJ, 510, 576

Pettini, M., Kellogg, M., Steidel, C. C., Dickinson, M., Adelberger, K. L., & Giavalisco, M. 1998, ApJ, 508, 539

Pettini, M., Steidel, C. C., Adelberger, K. L., Dickinson, M., & Giavalisco, M. 1999b, ApJ, in press, astro-ph/9908007

Pritchet, C. J. 1994, PASP, 106, 1052

Rawlings, S., Lacy, M., Blundell, K. M., Eales, S. A., Bunker, A. J., & Garrington, S. T. 1996, Nature, 383, 502

Rawlings, S. & Saunders, R. 1991, Nature, 349, 138

Rawlings, S., Saunders, R., Eales, S. A., & Mackay, C. 1989, MNRAS, 240, 701

Rees, M. J. 1995, PASP, 107, 1176

Richards, E. A. 1999, ApJ, 513, 9

Richards, E. A., Kellerman, K. I., Fomalont, E. B., Windhorst, R. A., & Partridge, R. B. 1998, AJ, 116, 1034

Rigler, M. A., Stockton, A., Lilly, S. J., Hammer, F., & Fevre, O. L. 1992, ApJ, 385, 61

Rosati, P. 1999, in *Wide Field Surveys in Cosmology*, ed. Y. Mellier & S. Colombi (Gif sur Yvette: Editions Frontières), in press

Rosati, P., Stanford, S. A., Eisenhardt, P. R., Elston, R., Spinrad, H., Stern, D., & Dey, A. 1999, AJ, 118, 76

Rowan-Robinson, M., Broadhurst, T. J., Lawrence, A., McMahon, R. G., & Lonsdale, C. J. 1991, Nature, 351, 719

Sanders, D. B. & Mirabel, I. F. 1996, ARA&A, 34, 749

Sawicki, M. J., Lin, H., & Yee, H. K. C. 1997, AJ, 113, 1

Sawicki, M. J. & Yee, H. K. C. 1998, AJ, 115, 1329

Schechter, P. 1976, ApJ, 203, 297

Schlegel, D., Finkbeiner, D., & Davis, M. 1998, ApJ, 500, 525

Schmidt, M., Hasinger, G., Gunn, J., Schneider, D., Burg, R., Giacconi, R., Lehmann, I., MacKenty, J., et al. 1998, A&A, 329, 495

Schneider, D. P., Schmidt, M., & Gunn, J. E. 1989, AJ, 98, 1507

—. 1991a, AJ, 101, 2004

—. 1991b, AJ, 102, 387

Shapiro, P. 1995, ApJS, 102, 191

Smail, I., Ivison, R., & Blain, A. 1997, ApJ, 490, L5

Smail, I., Ivison, R., Blain, A., & Kneib, J.-P. 1998, ApJ, 507, L21

Smith, H. E., Junkkarinen, V. T., Spinrad, H., Grueff, G., & Vigotti, M. 1979, ApJ, 231, 307

Smith, J. et al. 1994, AJ, 108, 1147

Somerville, R. S., Primack, J., & Faber, S. 1999, MNRAS, in press, astro-ph/9806228

Songaila, A., Cowie, L. L., Hu, E. M., & Gardner, J. P. 1994, ApJS, 94, 461

Songaila, A., Hu, E. M., Cowie, L. L., & McMahon, R. G. 1999, ApJ, in press, astro-ph/9908321

Spinrad, H. 1982, PASP, 94, 397

Spinrad, H., Dey, A., & Graham, J. R. 1995, ApJ, 438, L51

Spinrad, H., Dey, A., Stern, D., & Bunker, A. J. 1999, in *The Most Disant Radio Galaxies*, ed. H. Röttgering, P. N. Best, & M. D. Lehnert (Dordrecht: Kluwer), 257

Spinrad, H., Dey, A., Stern, D., Peacock, J. A., Dunlop, J., Jimenez, R., & Windhorst, R. A. 1997, ApJ, 484, 581

Spinrad, H. & Djorgovski, S. 1983, S&T, 65, 321

—. 1984, ApJ, 285, L49

Spinrad, H. & Smith, H. E. 1976, ApJ, 206, 355

Spinrad, H., Smith, H. E., Hunstead, R., & Ryle, M. 1975, ApJ, 198, 7

Spinrad, H., Stern, D., Bunker, A. J., Dey, A., Lanzetta, K., Yahil, A., Pascarelle, S., & Fernàndez-Soto, A. 1998, AJ, 116, 2617

Stanford, S. A., Eisenhardt, P. R. M., & Dickinson, M. 1995, ApJ, 450, 512

Stanford, S. A., Elston, R., Eisenhardt, P. R. M., Spinrad, H., Stern, D., & Dey, A. 1997, AJ, 114, 2232

Steidel, C. S. 2000, in *Photometric Redshifts and High-Redshift Galaxies*, ed. R. Weymann, L. Storrie-Lombardi, M. Sawicki, & R. Brunner (San Francisco: ASP Conference Series), in press

Steidel, C. S., Adelberger, K. L., Dickinson, M., Giavalisco, M., Pettini, M., & Kellogg, M. 1998, ApJ, 492, 428

Steidel, C. S., Adelberger, K. L., Giavalisco, M., Dickinson, M., & Pettini, M. 1999, ApJ, 519, 1

Steidel, C. S., Giavalisco, M., Dickinson, M., & Adelberger, K. L. 1996a, AJ, 112, 352

Steidel, C. S., Giavalisco, M., Pettini, M., Dickinson, M., & Adelberger, K. L. 1996b, ApJ, 462, 17

Steidel, C. S. & Hamilton, D. 1992, AJ, 104, 941

Steidel, C. S. & Sargent, W. L. W. 1987, ApJ, 313, 171

Stern, D., Bunker, A. J., Spinrad, H., & Dey, A. 1999a, ApJ, submitted

Stern, D., Bunker, A. J., Spinrad, H., Dey, A., Lanzetta, K., Yahil, A., Pascarelle, S., & Fernàndez-Soto, A. 2000, AJ, in preparation

Stern, D., Dey, A., Spinrad, H., Maxfield, L. M., Dickinson, M. E., Schlegel, D., & González, R. A. 1999b, AJ, 117, 1122

Stern, D. et al. 1999c, ApJ, in preparation

Tenorio-Tagle, G., Kunth, D., Terlevich, E., Terlevich, R., & Silich, S. A. 1999, MNRAS, in press, astro-ph/9905324

Teplitz, H. I., Malkan, M., & McLean, I. S. 1998, ApJ, 506, 519

Terlevich, E., Dìaz, A. I., Terlevich, R., & Garcìa, M. L. 1993, MNRAS, 260, 3

Thommes, E. 1999, in *From Stars to Galaxies to the Universe*, in press, astro-ph/9812223

Thommes, E., Meisenheimer, K., Fockenbrock, R., Hippelein, H., Röser, H. J., & Beckwith, S. 1998, MNRAS, 293, L6

Thompson, D. & Djorgovski, S. G. 1995, AJ, 110, 982

Thuan, T. X. & Izotov, Y. I. 1997, ApJ, 489, 623

Thuan, T. X., Izotov, Y. I., & Lipovetsky, V. A. 1997, ApJ, 477, 661

van Breugel, W., De Breuck, C., Stanford, S. A., Stern, D., Röttgering, H., & Miley, G. 1999, ApJ, 518, L61

van Breugel, W., Stanford, S. A., Spinrad, H., Stern, D., & Graham, J. R. 1998, ApJ, 502, 614

Waddington, I., Windhorst, R. A., Cohen, S. H., Partridge, R. B., Spinrad, H., & Stern, D. 1999, ApJ, in press, astro-ph/9910069

Wang, Y., Bahcall, N., & Turner, E. L. 1998, AJ, 116, 2081

Weymann, R., Stern, D., Bunker, A. J., Spinrad, H., Chaffee, F., Thompson, R., & Storrie-Lombardi, L. 1998, ApJ, 505, L95

White, S. D. M. 1997, in *The Early Universe with the VLT*, ed. J. Bergemon (Berlin: Springer), 219

Williams, R. E. et al. 1996, AJ, 112, 1335

Woosley, S. E. 1993, ApJ, 405, 273

Yan, L., McCarthy, P. J., Freudling, W., Teplitz, H. I., Malumuth, E. M., Weymann, R. J., & Malkan, M. A. 1999, ApJ, 519, L47

Yee, H. K. C. 1998, in *The Birth of Galaxies*, in press, astro-ph/9809347

Zamorani, G., Hasinger, G., Burg, R., Giacconi, R., & Schmidt, M. 1999, A&AS, 346

Zhang, Y., Anninos, P., Norman, M. L., & Meiksin, A. 1997, ApJ, 485, 496

Zuo, L. & Lu, L. 1993, ApJ, 418, 601

This figure "fig5.jpg" is available in "jpg" format from:

http://suriya.library.cornell.edu/ps/astro-ph/9912082

This figure "fig9.jpg" is available in "jpg" format from:

http://suriya.library.cornell.edu/ps/astro-ph/9912082